

48. *On the Stress Distribution in the Vicinity of  
a Horizontal Circular Hole in a Gravitating  
Wedge-Shaped Elastic Solid.*

By Genrokuro NISHIMURA and Takeo TAKAYAMA,

Earthquake Research Institute.

(Read May 17, 1932.—Received June 20, 1932.)

1. The problem of the stress distribution in the neighbourhood of a circular hole in a gravitating semi-infinite solid has recently been studied by N. Yamaguti<sup>1)</sup> and T. Sugihara<sup>2)</sup> independently. N. Yamaguti studied the case of a horizontal circular hole for the purpose of investigating the stability of a horizontal tunnel, and T. Sugihara discussed an inclined circular hole in relation to the mining engineering.

It may be of some importance to study the effect of topography on the stability of a tunnel, and the present paper shall make some contribution to this problem. The paper consists of two parts: in the first part we studied the equilibrium of a gravitating wedge-shaped solid having no hole in its interior, and the second part treated of the stress distribution in the vicinity of a horizontal circular tunnel in a gravitating wedge-shaped solid having the vertex of right-angle.

**Part I. The Equilibrium of a Gravitating Wedge-Shaped  
Elastic Solid.**

2. The stress distribution in a gravitating wedge-shaped solid without a hole was studied by M. Lévy<sup>3)</sup> and N. Mononobe,<sup>4)</sup> and others. Taking the earthquake intensity into account, Professor N. Mononobe discussed a technically important problem in relation to the construction of a gravity dam. Independent of above authors, we have obtained the stress distribution in a gravitating wedge-shaped solid as a preliminary calculation for the investigation of the effect of a hole on that solid.

---

1) N. YAMAGUTI, *Jour. Civil Eng.*, Tokyo, 15 (1929), 291.

2) T. SUGIHARA, *Jour. Mining Inst., Japan*, 47 (1931), 560, (in Japanese).

3) M. LÉVY, *C. R.*, Paris, 127 (1898), 10.

4) N. MONONOBE, *水理と土木*, 2 (1929) & 3 (1930).

We use the rectangular coordinates  $(x, y, z)$ , taking the positive sense of  $x$ -axis upward and  $y$ -axis horizontal. Let the origin  $o$  be at the vertex of a gravitating wedge-shaped solid of which the surfaces are defined by the following two equations :

$$\left. \begin{aligned} y &= -x \cot \varphi, \\ y &= x \cot \theta. \end{aligned} \right\} \dots (1)$$

Now the equations of equilibrium of the gravitating solid are expressed by the following forms :

$$\left. \begin{aligned} \frac{\partial \widehat{xx}}{\partial x} + \frac{\partial \widehat{xy}}{\partial y} &= \rho g, \\ \frac{\partial \widehat{xy}}{\partial x} + \frac{\partial \widehat{yy}}{\partial y} &= 0, \end{aligned} \right\} \dots (2)$$

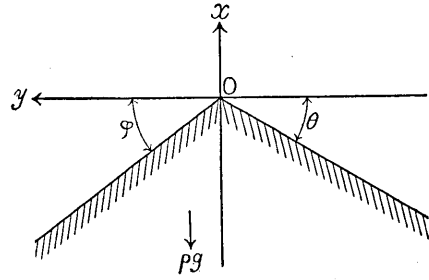


Fig. 1.

where  $\rho$  and  $g$  are the density and the gravity constant of the solid, and  $\widehat{xx}$ ,  $\widehat{yy}$ , the normal components of stress, and  $\widehat{xy}$  is the shearing component of stress.

The components of stress  $\widehat{xx}$ ,  $\widehat{yy}$ ,  $\widehat{xy}$  are expressed by the following relations :

$$\left. \begin{aligned} \widehat{xx} &= \lambda \left( \frac{\partial u}{\partial x} + \frac{\partial v}{\partial y} \right) + 2\mu \frac{\partial u}{\partial x}, \\ \widehat{yy} &= \lambda \left( \frac{\partial u}{\partial x} + \frac{\partial v}{\partial y} \right) + 2\mu \frac{\partial v}{\partial y}, \\ \widehat{xy} &= \mu \left( \frac{\partial v}{\partial x} - \frac{\partial u}{\partial y} \right), \end{aligned} \right\} \dots (3)$$

where  $u, v$  are the  $x$ - and  $y$ -components of displacement of the solid, and  $\lambda, \mu$  are the Lamé's elastic constants of that solid.

In equation (2), we substitute for the components of stress the expression (3); and we thus obtain the following equations :

$$\left. \begin{aligned} (\lambda + 2\mu) \frac{\partial \Delta}{\partial x} - 2\mu \frac{\partial \varpi}{\partial y} &= \rho g, \\ (\lambda + 2\mu) \frac{\partial \Delta}{\partial y} + 2\mu \frac{\partial \varpi}{\partial x} &= 0, \end{aligned} \right\} \dots (4)$$

where

$$\left. \begin{aligned} \Delta &= \frac{\partial u}{\partial x} + \frac{\partial v}{\partial y}, \\ 2\varpi &= \frac{\partial v}{\partial x} - \frac{\partial u}{\partial y} \end{aligned} \right\} \dots (5)$$

Now there are many particular solutions of (4), and we take the following forms of  $\Delta$  and  $2\pi$  satisfying (4) for the present study:

$$\left. \begin{aligned} \Delta &= A_0 + A_1x + A_2y, \\ 2\pi &= B_0 - \frac{(\lambda + 2\mu)}{\mu} A_2x + \frac{\{(\lambda + 2\mu)A_1 - \rho g\}}{\mu} y, \end{aligned} \right\} \dots\dots (6)$$

where  $A_0, B_0, A_1$  and  $A_2$  are the arbitrary constants to be determined by the boundary conditions of elasticity of the solid.

We can find the following two differential equations in relation to  $u, v, \Delta$  and  $2\pi$  from the relations (5):

$$\left. \begin{aligned} \frac{\partial^2 u}{\partial x^2} + \frac{\partial^2 u}{\partial y^2} &= \frac{\partial \Delta}{\partial x} - 2 \frac{\partial 2\pi}{\partial y}, \\ \frac{\partial^2 v}{\partial y^2} + \frac{\partial^2 v}{\partial x^2} &= \frac{\partial \Delta}{\partial y} + 2 \frac{\partial 2\pi}{\partial x}. \end{aligned} \right\} \dots\dots\dots (7)$$

Substituting the relations (6) for the expressions of  $\Delta$  and  $2\pi$  in the right-hand terms of the equations (7), we obtain the particular solutions of  $u$  and  $v$  as follows:

$$\left. \begin{aligned} u &= \frac{A_1}{2} x^2 - B_0 y - \frac{\{(\lambda + 2\mu)A_1 - \rho g\}}{2\mu} y^2, \\ v &= A_0 y + \frac{A_2}{2} y^2 - \frac{(\lambda + 2\mu)}{2\mu} A_2 x^2. \end{aligned} \right\} \dots\dots\dots (8)$$

As the complementary solutions  $u, v$  of (7), we take the following expressions which are favourable for the present study:

$$\left. \begin{aligned} u &= C_0 + C_1x + C_2y + C_3xy - \frac{C_4}{2} x^2 + \frac{C_4}{2} y^2, \\ v &= C_0' - C_1y + C_2x + C_4xy + \frac{C_3}{2} x^2 - \frac{C_3}{2} y^2, \end{aligned} \right\} \dots\dots\dots (9)$$

where  $C_0, C_0', C_1, C_2, C_3$  and  $C_4$  are also the arbitrary constants to be determined by the elasticity conditions. The expressions (8) and (9) satisfy, of course, the equations of equilibrium of the solid expressed by (4).

Using (6), (8) and (9), we obtain the following forms of the components of stress  $\widehat{xx}, \widehat{yy}, \widehat{xy}$  by the relations of (3);

$$\left. \begin{aligned} \widehat{xx} &= \lambda A_0 + 2\mu C_1 + (\lambda + 2\mu)A_1x + \lambda A_2y + 2\mu C_3y - 2\mu C_4x, \\ \widehat{yy} &= (\lambda + 2\mu)A_0 - 2\mu C_1 + \lambda A_1x + (\lambda + 2\mu)A_2y + 2\mu C_4x - 2\mu C_3y, \\ \widehat{xy} &= \mu(2C_2 - B_0) - (\lambda + 2\mu)A_2x - \{(\lambda + 2\mu)A_1 - \rho g\}y + 2\mu C_4y + 2\mu C_3x. \end{aligned} \right\} (10)$$

Now the two surfaces of the solid expressed by (1) are completely free from traction, and therefore the normal and shearing stresses in these two surfaces must be zero. Then, by these boundary conditions, we have the following equations in regard to the arbitrary constants :

$$A_0 = C_1 = C_2 = B_0 = 0, \dots\dots\dots(11)$$

$$\begin{aligned} & \{ \lambda \tan \varphi \sin^2 \varphi + 3(\lambda + 2\mu) \sin \varphi \cos \varphi \} A_1 + \{ \lambda \cos^2 \varphi \\ & + 3(\lambda + 2\mu) \sin^2 \varphi \} A_2 + 2\mu \{ \cos^2 \varphi - \sin^2 \varphi \} C_3 + 2\mu \tan \varphi \\ & \times \{ \sin^2 \varphi - 3 \cos^2 \varphi \} C_4 = \rho g \sin 2\varphi, \dots\dots\dots(12) \end{aligned}$$

$$\begin{aligned} & \{ (\lambda + 4\mu) \sin^2 \varphi - (\lambda + 2\mu) \cos^2 \varphi \} A_1 + \{ (\lambda + 2\mu) \sin^2 \varphi \tan \varphi \\ & - (\lambda + 4\mu) \cos^2 \varphi \tan \varphi \} A_2 + 2\mu \tan \varphi \{ 3 \cos^2 \varphi - \sin^2 \varphi \} C_3 \\ & + 2\mu \{ \cos^2 \varphi - 3 \sin^2 \varphi \} C_4 = -\rho g \cos 2\varphi, \dots\dots\dots(13) \end{aligned}$$

$$\begin{aligned} & \{ \lambda \sin^2 \theta + 3(\lambda + 2\mu) \cos^2 \theta \} \tan \theta A_1 - \{ 3(\lambda + 2\mu) \sin^2 \theta \\ & + \lambda \cos^2 \theta \} A_2 + 2\mu \{ 3 \sin^2 \theta - \cos^2 \theta \} C_3 \\ & + 2\mu \{ \sin^2 \theta - 3 \cos^2 \theta \} \tan \theta C_4 = \rho g \sin 2\theta, \dots\dots\dots(14) \end{aligned}$$

$$\begin{aligned} & \{ (\lambda + 4\mu) \sin^2 \theta - (\lambda + 2\mu) \cos^2 \theta \} A_1 + \{ (\lambda + 4\mu) \cos^2 \theta - \\ & - (\lambda + 2\mu) \sin^2 \theta \} \tan \theta A_2 - 2\mu \tan \theta \{ 3 \cos^2 \theta - \sin^2 \theta \} C_3 \\ & - 2\mu \{ 3 \sin^2 \theta - \cos^2 \theta \} C_4 = -\rho g \cos 2\theta. \dots\dots\dots(15) \end{aligned}$$

From these equations we can easily obtain  $A_1, A_2, C_3$  and  $C_4$ , and find the final results  $\widehat{xx}, \widehat{yy}, \widehat{xy}$  satisfying all elasticity conditions from the equations (10). These results are the most general ones for the gravitating wedge-shaped solid having any vertex angle.

For the special case where the vertex has right-angle as shewn in Fig. 2 in which the relation between the new axes  $OX, OY$  of the rectangular coordinates  $(X, Y)$  and the  $ox, oy$  is shewn, we can easily obtain the expressions as follows:

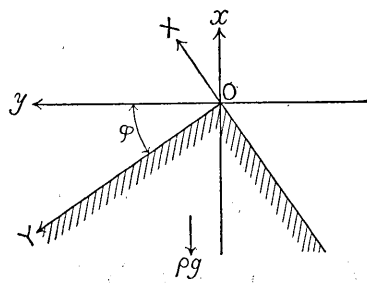


Fig. 2.

$$\left. \begin{aligned} \widehat{xx} &= (\lambda + 2\mu) \rho g \frac{\partial A_1}{\partial} x + \lambda \rho g \frac{\partial A_2}{\partial} y + 2\mu \rho g \frac{\partial C_3}{\partial} y - 2\rho g \frac{\partial C_4}{\partial} x, \\ \widehat{yy} &= \lambda \rho g \frac{\partial A_1}{\partial} x + (\lambda + 2\mu) \rho g \frac{\partial A_2}{\partial} y + 2\mu \rho g \frac{\partial C_4}{\partial} x - 2\mu \rho g \frac{\partial C_3}{\partial} y, \\ \widehat{xy} &= -(\lambda + 2\mu) \rho g \frac{\partial A_2}{\partial} x - \left\{ (\lambda + 2\mu) \frac{\partial A_1}{\partial} - 1 \right\} \rho g y + 2\mu \rho g \frac{\partial C_4}{\partial} y + 2\mu \rho g \frac{\partial C_3}{\partial} x, \end{aligned} \right\} (16)$$

$$\frac{\vartheta}{4\mu^2} = \left\{ \begin{array}{l} \{3(\lambda+2\mu)\cos\varphi\sin^2\varphi+\lambda\cos^3\varphi\}, \{3(\lambda+2\mu)\cos^2\varphi\sin\varphi+\lambda\sin^3\varphi\}, \\ \{\sin^3\varphi-3\sin\varphi\cos^2\varphi\}, \{\cos^3\varphi-3\sin^2\varphi\cos\varphi\} \\ \{-(\lambda+4\mu)\sin\varphi\cos^2\varphi+(\lambda+2\mu)\sin^3\varphi\}, \{(\lambda+4\mu)\cos\varphi\sin^2\varphi \\ -(\lambda+2\mu)\cos^3\varphi\}, \{\cos^3\varphi-3\cos\varphi\sin^2\varphi\}, \{3\sin\varphi\cos^2\varphi-\sin^3\varphi\} \\ \{-3(\lambda+2\mu)\cos^2\varphi\sin\varphi-\lambda\sin^3\varphi\}, \{3(\lambda+2\mu)\cos\varphi\sin^2\varphi+\lambda\cos^3\varphi\}, \\ \{\cos^3\varphi-3\sin^2\varphi\cos\varphi\}, \{-\sin^3\varphi+3\sin\varphi\cos^2\varphi\} \\ \{(\lambda+4\mu)\sin^2\varphi\cos\varphi-(\lambda+2\mu)\cos^3\varphi\}, \{(\lambda+4\mu)\sin\varphi\cos^2\varphi \\ -(\lambda+2\mu)\sin^3\varphi\}, \{-3\sin\varphi\cos^2\varphi+\sin^3\varphi\}, \{-3\cos\varphi\sin^2\varphi+\cos^3\varphi\} \end{array} \right. \quad (17)$$

$$\frac{\vartheta_{A1}}{4\mu^2} = \left\{ \begin{array}{l} 2\sin^2\varphi\cos\varphi, \{3(\lambda+2\mu)\cos^2\varphi\sin\varphi+\lambda\sin^3\varphi\}, \\ \{\sin^3\varphi-3\sin\varphi\cos^2\varphi\}, \{\cos^3\varphi-3\sin^2\varphi\cos\varphi\} \\ -\sin\varphi(\cos^2\varphi-\sin^2\varphi), \{(\lambda+4\mu)\cos\varphi\sin^2\varphi-(\lambda+2\mu)\cos^3\varphi\}, \\ \{\cos^3\varphi-3\cos\varphi\sin^2\varphi\}, \{3\sin\varphi\cos^2\varphi-\sin^3\varphi\} \\ -2\sin\varphi\cos^2\varphi, \{3(\lambda+2\mu)\cos\varphi\sin^2\varphi+\lambda\cos^3\varphi\}, \\ \{\cos^3\varphi-3\sin^2\varphi\cos\varphi\}, \{-\sin^3\varphi+3\sin\varphi\cos^2\varphi\} \\ -\cos\varphi(\cos^2\varphi-\sin^2\varphi), \{(\lambda+4\mu)\sin\varphi\cos^2\varphi-(\lambda+2\mu)\sin^3\varphi\} \\ \{-3\sin\varphi\cos^2\varphi+\sin^3\varphi\}, \{-3\cos\varphi\sin^2\varphi+\cos^3\varphi\}, \end{array} \right. \quad (18)$$

$$\frac{\vartheta_{A2}}{4\mu^2} = \left\{ \begin{array}{l} \{3(\lambda+2\mu)\cos\varphi\sin^2\varphi+\lambda\cos^3\varphi\}, 2\sin^2\varphi\cos\varphi, \\ \{\sin^3\varphi-3\sin\varphi\cos^2\varphi\}, \{\cos^3\varphi-3\sin^2\varphi\cos\varphi\} \\ \{-(\lambda+4\mu)\sin\varphi\cos^2\varphi+(\lambda+2\mu)\sin^3\varphi\}, -\sin\varphi(\cos^2\varphi-\sin^2\varphi), \\ \{\cos^3\varphi-3\cos\varphi\sin^2\varphi\}, \{3\sin\varphi\cos^2\varphi-\sin^3\varphi\} \\ \{-3(\lambda+2\mu)\cos^2\varphi\sin\varphi-\lambda\sin^3\varphi\}, -2\sin\varphi\cos^2\varphi, \\ \{\cos^3\varphi-3\sin^2\varphi\cos\varphi\}, \{-\sin^3\varphi+3\sin\varphi\cos^2\varphi\} \\ \{(\lambda+4\mu)\sin^2\varphi\cos\varphi-(\lambda+2\mu)\cos^3\varphi\}, -\cos\varphi(\cos^2\varphi-\sin^2\varphi), \\ \{-3\sin\varphi\cos^2\varphi+\sin^3\varphi\}, \{-3\cos\varphi\sin^2\varphi+\cos^3\varphi\}, \end{array} \right. \quad (19)$$

$$\frac{\vartheta_{C3}}{2\mu} = \left\{ \begin{array}{l} \{3(\lambda+2\mu)\cos\varphi\sin^2\varphi+\lambda\cos^3\varphi\}, \{3(\lambda+2\mu)\cos^2\varphi\sin\varphi+\lambda\sin^3\varphi\}, \\ 2\sin^2\varphi\cos\varphi, \{\cos^3\varphi-3\sin^2\varphi\cos\varphi\} \\ \{-(\lambda+4\mu)\sin\varphi\cos^2\varphi+(\lambda+2\mu)\sin^3\varphi\}, \{(\lambda+4\mu)\cos\varphi\sin^2\varphi \\ -(\lambda+2\mu)\cos^3\varphi\}, -\sin\varphi(\cos^2\varphi-\sin^2\varphi), \{3\sin\varphi\cos^2\varphi-\sin^3\varphi\} \\ \{-3(\lambda+2\mu)\cos^2\varphi\sin\varphi-\lambda\sin^3\varphi\}, \{3(\lambda+2\mu)\cos\varphi\sin^2\varphi+\lambda\cos^3\varphi\}, \\ -2\sin\varphi\cos^2\varphi, \{-\sin^3\varphi+3\sin\varphi\cos^2\varphi\} \\ \{(\lambda+4\mu)\sin^2\varphi\cos\varphi-(\lambda+2\mu)\cos^3\varphi\}, \{(\lambda+4\mu)\sin\varphi\cos^2\varphi \\ -(\lambda+2\mu)\sin^3\varphi\}, -\cos\varphi(\cos^2\varphi-\sin^2\varphi), \{-3\cos\varphi\sin^2\varphi+\cos^3\varphi\} \end{array} \right. \quad (20)$$

$$\frac{\vartheta_{C_4}}{2\mu} = \left\{ \begin{array}{l} \{3(\lambda + 2\mu) \cos \varphi \sin^2 \varphi + \lambda \cos^3 \varphi\}, \{3(\lambda + 2\mu) \cos^2 \varphi \sin \varphi + \lambda \sin^3 \varphi\}, \\ \{\sin^3 \varphi - 3 \sin \varphi \cos^2 \varphi\}, 2 \sin^2 \varphi \cos \varphi \\ \{-(\lambda + 4\mu) \sin \varphi \cos^2 \varphi + (\lambda + 2\mu) \sin^3 \varphi\}, \{(\lambda + 4\mu) \cos \varphi \sin^2 \varphi \\ -(\lambda + 2\mu) \cos^3 \varphi\}, \{\cos^3 \varphi - 3 \cos \varphi \sin^2 \varphi\}, -\sin \varphi \{\cos^2 \varphi - \sin^2 \varphi\} \\ \{-3(\lambda + 2\mu) \cos^2 \varphi \sin \varphi - \lambda \sin^3 \varphi\}, \{3(\lambda + 2\mu) \cos \varphi \sin^2 \varphi + \lambda \cos^3 \varphi\}, \\ \{\cos^3 \varphi - 3 \sin^2 \varphi \cos \varphi\}, -2 \sin \varphi \cos^2 \varphi \\ \{(\lambda + 4\mu) \sin^2 \varphi \cos \varphi - (\lambda + 2\mu) \cos^3 \varphi\}, \{(\lambda + 4\mu) \sin \varphi \cos^2 \\ -(\lambda + 2\mu) \sin^3 \varphi\}, \{-3 \sin \varphi \cos^2 \varphi + \sin^3 \varphi\}, -\cos \varphi \{\cos^2 \varphi - \sin^2 \varphi\} \end{array} \right. \quad (21)$$

For ascertaining the stress distribution in the solid we take a numerical example. Assuming  $\lambda = \mu$  (Poisson's ratio = 1/4), we calculate  $\vartheta$ ,  $\vartheta_{A_1}$ ,  $\vartheta_{A_2}$ ,  $\vartheta_{C_3}$  and  $\vartheta_{C_4}$  in accordance with the various magnitudes of angle  $\varphi$ ; and the results are tabulated in the following table. (Table I.)

Table I.

$\varphi$	0°	20°	30°	45°	60°	70°	90°
$\frac{\vartheta_{A_1}}{\vartheta}$	$\frac{1}{4} \frac{\rho g}{\mu}$	$\frac{1}{4} \frac{\rho g}{\mu}$	$\frac{1}{4} \frac{\rho g}{\mu}$	$\frac{1}{4} \frac{\rho g}{\mu}$	$\frac{1}{4} \frac{\rho g}{\mu}$	$\frac{1}{4} \frac{\rho g}{\mu}$	$\frac{1}{4} \frac{\rho g}{\mu}$
$\frac{\vartheta_{A_2}}{\vartheta}$	0	0	0	0	0	0	0
$\frac{\vartheta_{C_3}}{\vartheta}$	0	$0.123 \frac{\rho g}{\mu}$	$0.108 \frac{\rho g}{\mu}$	0	$-0.108 \frac{\rho g}{\mu}$	$-0.123 \frac{\rho g}{\mu}$	0
$\frac{\vartheta_{C_4}}{\vartheta}$	$-\frac{1}{8} \frac{\rho g}{\mu}$	$-0.0219 \frac{\rho g}{\mu}$	$0.062 \frac{\rho g}{\mu}$	$\frac{1}{8} \frac{\rho g}{\mu}$	$0.062 \frac{\rho g}{\mu}$	$-0.0210 \frac{\rho g}{\mu}$	$-\frac{1}{8} \frac{\rho g}{\mu}$

Using the expressions (16) and Table I, we obtain the stress components  $\widehat{xx}$ ,  $\widehat{yy}$ ,  $\widehat{xy}$  as shewn in Table II and Fig. 3a, 3b, 3c.

Table II.

(unit =  $\rho g$ )

$\varphi$	0°	20°	30°	45°	60°	70°	90°
$\widehat{xx}$	$x$	$0.794x + 0.246y$	$0.626x + 0.216y$	$0.5x$	$0.626x - 0.216y$	$0.794x - 0.246y$	$x$
$\widehat{yy}$	0	$0.206x - 0.246y$	$0.374x - 0.216y$	$0.5x$	$0.374x + 0.216y$	$0.206x + 0.246y$	0
$\widehat{xy}$	0	$0.246x + 0.206y$	$0.216x + 0.374y$	$0.5y$	$-0.216x + 0.374y$	$-0.246x + 0.206y$	0

In Fig. 3a, 3b, and 3c, the abscissae shew the angle  $\varphi$  and the ordinates the magnitudes of the  $x$ - and  $y$ -components of the components of stress  $\widehat{xx}$ ,  $\widehat{yy}$ ,  $\widehat{xy}$  respectively. In Fig. 3a,  $\widehat{xx}(x)$  and  $\widehat{xx}(y)$  represent the  $x$ - and  $y$ -components of stress  $\widehat{xx}$  respectively, and therefore the magnitude of  $\widehat{xx}$  at any point in the solid is given by the algebraic sum of  $\widehat{xx}(x)$  and  $\widehat{xx}(y)$ .

From Table II, we can easily calculate the tangential components of stress  $\widehat{Y}Y$  on the surface  $OY$  of the solid :

$$\widehat{Y}Y_{on\ or} = -\rho g Y \sin \varphi. \dots (22)$$

This form is simple to know effect of  $\varphi$  on the properties of tangential stress  $\widehat{Y}Y$ . The compression stress only exists on the surface  $OY$ .

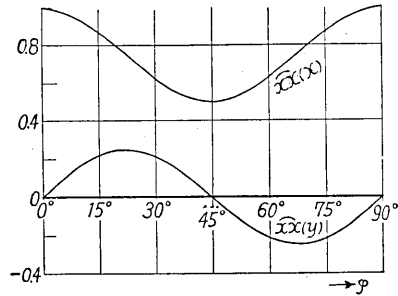


Fig. 3 a.

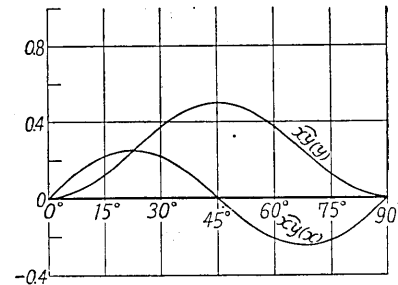


Fig. 3 b.

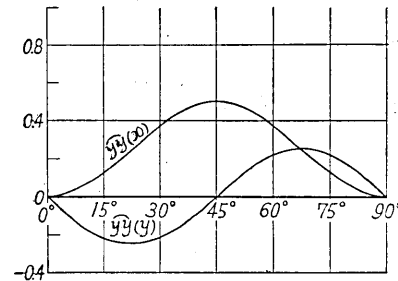


Fig. 3 c.

**Part II. The Stress Distribution in the Vicinity of a Horizontal Circular Hole in a Gravitating Wedge-Shaped Solid.**

3. In this part we studied the stress distribution in the vicinity of a horizontal hole of which the radius is  $a$ , and the centre  $O'$  is at the point  $(x = -\xi, y = \eta)$  as shewn in Fig. 4.

The vertex angle of the solid is assumed to be right-angle for the sake of simplicity as in the preceding section.

Now we must first obtain the general expressions of stresses which satisfy the equations of equilibrium of the solid. Using the cylindrical coordinates  $(r, \theta, z)$ , of which the axis  $z$  is coincident with the axis of the circular hole and the azimuthal angle  $\theta$  is taken counterclockwise from the axis  $o'x'$  as shewn in Fig. 4, we have the equations of equi-

rium of a gravitating solid :

$$\left. \begin{aligned} \frac{\partial \widehat{r r}}{\partial r} + \frac{1}{r} \frac{\partial \widehat{r \theta}}{\partial \theta} + \frac{\widehat{r r} - \widehat{\theta \theta}}{r} &= \rho g \cos \theta, \\ \frac{\partial \widehat{r \theta}}{\partial r} + \frac{1}{r} \frac{\partial \widehat{\theta \theta}}{\partial \theta} + 2 \frac{\widehat{r \theta}}{r} &= -\rho g \sin \theta. \end{aligned} \right\} \dots (23)$$

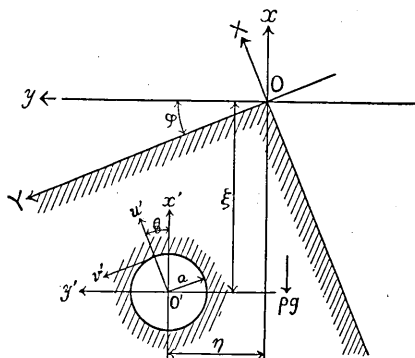


Fig. 4.

The normal components of stress  $\widehat{r r}$ ,  $\widehat{\theta \theta}$  and the shearing component  $\widehat{r \theta}$  are expressed by the radial and tangential components of displacement  $u, v$  in the forms :

$$\left. \begin{aligned} \widehat{r r} &= \lambda \left\{ \frac{1}{r} \frac{\partial}{\partial r} (r u') + \frac{1}{r} \frac{\partial v'}{\partial \theta} \right\} + 2 \mu \frac{\partial u'}{\partial r}, \\ \widehat{\theta \theta} &= \lambda \left\{ \frac{1}{r} \frac{\partial}{\partial r} (r u') + \frac{1}{r} \frac{\partial v'}{\partial \theta} \right\} + 2 \mu \left\{ \frac{1}{r} \frac{\partial v'}{\partial \theta} + \frac{u'}{r} \right\}, \\ \widehat{r \theta} &= \mu \left\{ \frac{\partial v'}{\partial r} - \frac{v'}{r} + \frac{1}{r} \frac{\partial u'}{\partial \theta} \right\}. \end{aligned} \right\} \dots (24)$$

To obtain the equation (23) we neglect the axial variation of stress, because the circular hole is horizontal.

In equation (23), we substitute for the components of stress the expression (24) ; and we thus obtain the following equations :

$$\left. \begin{aligned} (\lambda + 2\mu) \frac{\partial \Delta'}{\partial r} - \frac{2\mu}{r} \frac{\partial \varpi'}{\partial \theta} &= \rho g \cos \theta, \\ (\lambda + 2\mu) \frac{1}{r} \frac{\partial \Delta'}{\partial \theta} + 2\mu \frac{\partial \varpi'}{\partial r} &= -\rho g \sin \theta, \end{aligned} \right\} \dots (25)$$

where

$$\left. \begin{aligned} \Delta' &= \frac{\partial u'}{\partial r} + \frac{u'}{r} + \frac{1}{r} \frac{\partial v'}{\partial \theta}, \\ 2\varpi' &= \frac{\partial v'}{\partial r} + \frac{v'}{r} - \frac{1}{r} \frac{\partial u'}{\partial \theta}. \end{aligned} \right\} \dots (26)$$

Among the particular solutions satisfying (25), we take the particular solution which is useful for the present study as follows :

$$\left. \begin{aligned} \Delta' &= 0, \\ 2\varpi' &= -\frac{\rho g}{\mu} r \sin \theta. \end{aligned} \right\} \dots (27)$$



Next we must obtain the complementary solutions of (25) which are necessary to satisfy the boundary conditions of the solid.

Now the equations (25) give us the following equation :

$$\frac{\partial^2 \Delta'}{\partial r^2} + \frac{1}{r} \frac{\partial \Delta'}{\partial r} + \frac{\partial^2 \Delta'}{r^2 \partial \theta^2} = 0, \dots\dots\dots(28)$$

the solutions of which are expressed by

$$\begin{aligned} \Delta' = & B_0 + \left\{ \frac{F_1}{r} + B_1 r + \frac{C_1}{r} \right\} \cos \theta + \left\{ B_2 r^2 + C_2 \frac{1}{r^2} \right\} \cos 2\theta \\ & + \left\{ B_3 r^3 + \frac{C_3}{r^3} \right\} \cos 3\theta + \left\{ D_1 r + \frac{E_1}{r} \right\} \sin \theta + \left\{ D_2 r^2 + \frac{E_2}{r^2} \right\} \sin 2\theta \\ & + \left\{ D_3 r^3 + \frac{E_3}{r^3} \right\} \sin 3\theta, \dots\dots\dots(29) \end{aligned}$$

where  $B_0, B_1, C_1, B_2, C_2, B_3, C_3, F_1, D_1, E_1, D_2, E_2, D_3$  and  $E_3$  are the arbitrary constants to be determined by the elasticity conditions.

Using (29) we obtain the expressions of  $2\pi'$  which are the particular solutions of (25) as follows :

$$\begin{aligned} 2\pi' = & \left\{ \frac{(\lambda + 2\mu)}{\mu} B_1 r + \frac{(\lambda + 2\mu)}{\mu} C_1 \frac{1}{r} \right\} \sin \theta + \left\{ \frac{(\lambda + 2\mu)}{\mu} B_2 r^2 \right. \\ & + \left. \frac{(\lambda + 2\mu)}{\mu} C_2 \frac{1}{r^2} \right\} \sin 2\theta + \left\{ \frac{(\lambda + 2\mu)}{\mu} B_3 r^3 + \frac{(\lambda + 2\mu)}{\mu} \frac{C_3}{r^3} \right\} \sin 3\theta \\ & - \left\{ \frac{(\lambda + 2\mu)}{\mu} D_1 r + \frac{(\lambda + 2\mu)}{\mu} E_1 \frac{1}{r} \right\} \cos \theta - \left\{ \frac{(\lambda + 2\mu)}{\mu} D_2 r^2 \right. \\ & + \left. \frac{(\lambda + 2\mu)}{\mu} \frac{E_2}{r^2} \right\} \cos 2\theta - \left\{ \frac{(\lambda + 2\mu)}{\mu} D_3 r^3 + \frac{(\lambda + 2\mu)}{\mu} \frac{E_3}{r^3} \right\} \cos 3\theta. \\ & \dots\dots\dots(30) \end{aligned}$$

After some reductions we obtain the following the differential equations in relation to  $u', v'$  and  $\Delta', 2\pi'$  from the relations expressed by (26) :

$$\frac{\partial^2 (ru')}{\partial r^2} + \frac{1}{r} \frac{\partial (ru')}{\partial r} + \frac{1}{r^2} \frac{\partial^2 ru'}{\partial \theta^2} = \frac{1}{r} \frac{\partial (r^2 \Delta')}{\partial r} - 2 \frac{\partial \pi'}{\partial \theta}, \dots\dots(31)$$

$$\frac{\partial^2 (rv')}{\partial r^2} + \frac{1}{r} \frac{\partial (rv')}{\partial r} + \frac{1}{r^2} \frac{\partial^2 (rv')}{\partial \theta^2} = \frac{\partial \Delta'}{\partial \theta} + \frac{2}{r} \frac{\partial (r\pi')}{\partial r}. \dots\dots(32)$$

Substituting (27) for the expressions of  $\Delta'$  and  $2\pi'$  in the equations (31), (32), we obtain the particular solutions of (31) and (32) as follows :

$$\left. \begin{aligned} u' &= \frac{\rho g}{8\mu} r^2 \cos \theta, \\ v' &= -\frac{3\rho g}{8\mu} r^2 \sin \theta. \end{aligned} \right\} \dots\dots\dots (33)$$

These expressions satisfy, of course, the equilibrium equations (25).

Substituting (29) and (30) for the expressions of  $\mathcal{A}'$  and  $2\omega'$  in the right-hand terms of the equations (31) and (32), we obtain the particular solutions which are, of course, the particular solutions of (25) in the following forms :

$$\left. \begin{aligned} u' &= \frac{1}{2} B_0 r + \left[ \frac{(-\lambda + \mu)}{8\mu} B_1 r^2 + \left\{ \frac{(\lambda + 3\mu)}{2\mu} \ln \frac{r}{a} + \frac{1}{2} \right\} F_1 \right] \cos \theta \\ &\quad - \left\{ \frac{\lambda}{6\mu} B_2 r^3 + \frac{(\lambda + 2\mu)}{2\mu} \frac{C_2}{r} \right\} \cos 2\theta - \left\{ \frac{(3\lambda + \mu)}{16\mu} B_3 r^4 \right. \\ &\quad \left. + \frac{(3\lambda + 5\mu)}{8\mu} \frac{C_3}{r^2} \right\} \cos 3\theta + \frac{(-\lambda + \mu)}{8\mu} D_1 r^2 \sin \theta - \left\{ \frac{\lambda}{6\mu} D_2 r^3 \right. \\ &\quad \left. + \frac{(\lambda + 2\mu)}{2\mu} \frac{E_2}{r} \right\} \sin 2\theta - \left\{ \frac{(3\lambda + \mu)}{16\mu} D_3 r^4 + \frac{(3\lambda + 5\mu)}{8\mu} \frac{E_3}{r^2} \right\} \sin 3\theta, \\ v' &= \left[ \frac{(3\lambda + 5\mu)}{8\mu} B_1 r^2 - \left\{ \frac{(\lambda + 3\mu)}{2\mu} \ln \frac{r}{a} + \frac{(\lambda + 2\mu)}{2\mu} \right\} F_1 \right] \sin \theta \\ &\quad + \left\{ \frac{(2\lambda + 3\mu)}{6\mu} B_2 r^3 + \frac{1}{2} \frac{C_2}{r} \right\} \sin 2\theta + \left\{ \frac{(5\lambda + 7\mu)}{16\mu} B_3 r^4 \right. \\ &\quad \left. - \frac{(\lambda - \mu)}{8\mu} \frac{C_3}{r^2} \right\} \sin 3\theta - \frac{(3\lambda + 5\mu)}{8\mu} D_1 r^2 \cos \theta - \left\{ \frac{(2\lambda + 3\mu)}{6\mu} D_2 r^3 \right. \\ &\quad \left. + \frac{1}{2} \frac{E_2}{r} \right\} \cos 2\theta - \left\{ \frac{(5\lambda + 7\mu)}{16\mu} D_3 r^4 - \frac{(\lambda - \mu)}{8\mu} \frac{E_3}{r^2} \right\} \cos 3\theta. \end{aligned} \right\} (34)$$

As the complementary solutions of (31) and (32) which are favourable to the present study, we obtain the following  $u'$  and  $v'$  ;

$$\left. \begin{aligned} u' &= \frac{B_0''}{r} + \frac{C_1''}{r^2} \cos \theta + \left\{ B_2'' r + \frac{C_2''}{r^3} \right\} \cos 2\theta + \left\{ B_3'' r^2 + \frac{C_3''}{r^4} \right\} \cos 3\theta \\ &\quad + \frac{D_1''}{r^2} \sin \theta + \left\{ D_2'' r + \frac{E_2''}{r^3} \right\} \sin 2\theta + \left\{ D_3'' r^2 + \frac{E_3''}{r^4} \right\} \sin 3\theta, \\ v' &= \frac{C_1''}{r^2} \sin \theta - \left\{ B_2'' r - \frac{C_2''}{r^3} \right\} \sin 2\theta - \left\{ B_3'' r^2 - \frac{C_3''}{r^4} \right\} \sin 3\theta \\ &\quad - \frac{D_1''}{r^2} \cos \theta + \left\{ D_2'' r - \frac{E_2''}{r^3} \right\} \cos 2\theta + \left\{ D_3'' r^2 - \frac{E_3''}{r^4} \right\} \cos 3\theta. \end{aligned} \right\} (35)$$

The general expressions of the components of the displacement thus obtained, (33), (34) and (35), satisfy, of course, the equations of equilibrium of the elastic solid (25). Using these general expressions we get the general expressions of stress  $\widehat{rr}$ ,  $\widehat{\theta\theta}$ , and  $\widehat{r\theta}$  as in the following forms :

$$\begin{aligned} \widehat{rr} = & (\lambda + \mu)B_0 - 2\mu \frac{B_0''}{r^2} + \left[ \frac{1}{2} \rho g r + \frac{(\lambda + \mu)}{2} B_1 r - \frac{4\mu}{r^3} C_1'' + \frac{(2\lambda + 3\mu)}{r} F_1 \right] \cos \theta \\ & + \left[ 2\mu B_2'' + \frac{2(\lambda + \mu)}{r^2} C_2 - \frac{6\mu}{r^4} C_2'' \right] \cos 2\theta + \left[ -\frac{(\lambda + \mu)}{2} B_3 r^3 + 4\mu B_3'' r \right. \\ & + \left. \frac{5(\lambda + \mu)}{2} \frac{C_3}{r^3} - \frac{8\mu}{r^5} C_3'' \right] \cos 3\theta + \left[ \frac{(\lambda + \mu)}{2} D_1 r + \frac{(2\lambda + 3\mu)}{r} E_1 - \frac{4\mu}{r^3} E_1'' \right] \sin \theta \\ & + \left[ 2\mu D_2'' + \frac{2(\lambda + \mu)}{r^2} E_2 - \frac{6\mu}{r^4} E_2'' \right] \sin 2\theta + \left[ -\frac{(\lambda + \mu)}{2} r^3 D_3 + 4\mu D_3'' r \right. \\ & + \left. \frac{5(\lambda + \mu)}{2r^3} E_3 - \frac{8\mu}{r^5} E_3'' \right] \sin 3\theta, \dots \dots \dots (36) \end{aligned}$$

$$\begin{aligned} \widehat{\theta\theta} = & (\lambda + \mu)B_0 + 2\mu \frac{B_0''}{r^2} + \left[ \frac{3}{2} (\lambda + \mu) B_1 r - \frac{\rho g}{2} r + \frac{4\mu}{r^3} C_1'' - \frac{\mu}{r} F_1 \right] \cos \theta \\ & + \left[ 2(\lambda + \mu) B_2 r^2 - 2\mu B_2'' + \frac{6\mu}{r^4} C_2'' \right] \cos 2\theta + \left[ \frac{5}{2} (\lambda + \mu) B_3 r^3 - 4\mu B_3'' r \right. \\ & - \left. \frac{(\lambda + \mu)}{2} \frac{C_3}{r^3} + \frac{8\mu}{r^5} C_3'' \right] \cos 3\theta + \left[ \frac{3}{2} (\lambda + \mu) D_1 r - \frac{\mu}{r} E_1 + \frac{4\mu}{r^3} E_1'' \right] \sin \theta \\ & + \left[ 2(\lambda + \mu) D_2 r^2 - 2\mu D_2'' + \frac{6\mu}{r^4} E_2'' \right] \sin 2\theta + \left[ \frac{5}{2} (\lambda + \mu) D_3 r^3 - 4\mu D_3'' r \right. \\ & - \left. \frac{(\lambda + \mu)}{2} \frac{E_3}{r^3} + \frac{8\mu}{r^5} E_3'' \right] \sin 3\theta, \dots \dots \dots (37) \end{aligned}$$

$$\begin{aligned} \widehat{r\theta} = & \left[ -\frac{\rho g r}{2} + \frac{(\lambda + \mu)}{2} B_1 r - \frac{4\mu}{r^3} C_1'' - \frac{\mu}{r} F_1 \right] \sin \theta + \left[ (\lambda + \mu) B_2 r^2 - 2\mu B_2'' \right. \\ & + \left. (\lambda + \mu) \frac{C_2}{r^2} - \frac{6\mu}{r^4} C_2'' \right] \sin 2\theta + \left[ \frac{3(\lambda + \mu)}{2} B_3 r^3 - 4\mu B_3'' r \right. \\ & + \left. \frac{3}{2} \frac{(\lambda + \mu)}{r^3} C_3 - \frac{8\mu}{r^5} C_3'' \right] \sin 3\theta + \left[ -\frac{(\lambda + \mu)}{2} D_1 r + \frac{\mu}{r} E_1 + \frac{4\mu}{r^3} E_1'' \right] \cos \theta \\ & + \left[ -(\lambda + \mu) r^2 D_2 + 2\mu D_2'' - (\lambda + \mu) \frac{E_2}{r^2} + \frac{6\mu}{r^4} E_2'' \right] \cos 2\theta \\ & + \left[ -\frac{3(\lambda + \mu)}{2} D_3 r^3 + 4\mu D_3'' r - \frac{3}{2} \frac{(\lambda + \mu)}{r^3} E_3 + \frac{8\mu}{r^5} E_3'' \right] \cos 3\theta \dots \dots (38) \end{aligned}$$

These expressions of the components of stress satisfy, of course, the equations of equilibrium of the solid under the gravitating field expressed

by (23). Using these expressions of traction we shall study the stresses in the vicinity of a horizontal hole in the wedge-shaped solid of which the vertex has right-angle. We have obtained the expressions (16) of the stress distribution in the wedge-shaped solid having the vertex of right-angle in the preceding section. When we transform these components of stress  $\widehat{xx}$ ,  $\widehat{yy}$ ,  $\widehat{xy}$  into the components of stress  $\widehat{rr}$ ,  $\widehat{\theta\theta}$ ,  $\widehat{r\theta}$  in the cylindrical coordinates  $(r, \theta)$  of which the relation with the rectangular coordinates  $(x', y')$  has already been explained, we have the following forms :

$$\begin{aligned} \widehat{rr} = & \left[ -(\lambda + \mu) \rho g \xi \frac{\partial_{A1}}{\partial} + (\lambda + \mu) \rho g \eta \frac{\partial_{A2}}{\partial} \right] + \left[ \frac{(\lambda + \mu)}{2} \rho g \frac{\partial_{A1}}{\partial} + \frac{\rho g}{2} \right] r \cos \theta \\ & + \left[ \left\{ -\mu \frac{\partial_{A1}}{\partial} + 2\mu \frac{\partial_{C4}}{\partial} \right\} \xi + \left\{ -\mu \frac{\partial_{A2}}{\partial} + 2\mu \frac{\partial_{C3}}{\partial} \right\} \eta \right] \rho g \cos 2\theta \\ & + \left[ \frac{(\lambda + 3\mu)}{2} \frac{\partial_{A1}}{\partial} - 2\mu \frac{\partial_{C4}}{\partial} - \frac{\rho g}{2} \right] \rho g r \cos 3\theta + \frac{(3\lambda + 4\mu)}{4} \frac{\partial_{A2}}{\partial} \rho g r \sin \theta \\ & + \left[ \left\{ (\lambda + 2\mu) \frac{\partial_{A2}}{\partial} - 2\mu \frac{\partial_{C3}}{\partial} \right\} \xi + \left\{ -(\lambda + 2\mu) \frac{\partial_{A1}}{\partial} + 2\mu \frac{\partial_{C4}}{\partial} + 1 \right\} \eta \right] \rho g \sin 2\theta \\ & + \left[ -\frac{(\lambda + 3\mu)}{2} \frac{\partial_{A2}}{\partial} + 2\mu \frac{\partial_{C3}}{\partial} \right] \rho g r \sin 3\theta, \dots\dots\dots(39) \end{aligned}$$

$$\begin{aligned} \widehat{\theta\theta} = & \left[ -(\lambda + \mu) \frac{\partial_{A1}}{\partial} \xi + (\lambda + \mu) \frac{\partial_{A2}}{\partial} \eta \right] \rho g + \left[ \frac{3}{2} (\lambda + \mu) \frac{\partial_{A1}}{\partial} - \frac{1}{2} \right] \rho g r \cos \theta \\ & + \left[ \left\{ \mu \frac{\partial_{A1}}{\partial} - 2\mu \frac{\partial_{C4}}{\partial} \right\} \xi + \left\{ \mu \frac{\partial_{A2}}{\partial} - 2\mu \frac{\partial_{C3}}{\partial} \right\} \eta \right] \rho g \cos 2\theta \\ & + \left[ -\frac{(\lambda + 3\mu)}{2} \frac{\partial_{A1}}{\partial} + 2\mu \frac{\partial_{C4}}{\partial} + \frac{1}{2} \right] \rho g r \cos 3\theta + \frac{3(\lambda + \mu)}{2} \frac{\partial_{A2}}{\partial} \rho g r \sin \theta \\ & - \left[ \left\{ (\lambda + 2\mu) \frac{\partial_{A2}}{\partial} - 2\mu \frac{\partial_{C3}}{\partial} \right\} \xi + \left\{ -(\lambda + 2\mu) \frac{\partial_{A1}}{\partial} + 2\mu \frac{\partial_{C4}}{\partial} + 1 \right\} \eta \right] \rho g \sin 2\theta \\ & + \left[ \frac{(\lambda + 3\mu)}{2} \frac{\partial_{A2}}{\partial} - 2\mu \frac{\partial_{C3}}{\partial} \right] \rho g r \sin 3\theta, \dots\dots\dots(40) \end{aligned}$$

$$\begin{aligned} \widehat{r\theta} = & \left[ \frac{(\lambda + \mu)}{2} \frac{\partial_{A1}}{\partial} - \frac{1}{2} \right] \rho g r \sin \theta \\ & + \left[ \left\{ \mu \frac{\partial_{A1}}{\partial} - 2\mu \frac{\partial_{C4}}{\partial} \right\} \xi + \left\{ \mu \frac{\partial_{A2}}{\partial} - 2\mu \frac{\partial_{C3}}{\partial} \right\} \eta \right] \rho g \sin 2\theta \\ & + \left[ -\frac{(\lambda + 3\mu)}{2} \frac{\partial_{A1}}{\partial} + 2\mu \frac{\partial_{C4}}{\partial} + \frac{1}{2} \right] \rho g r \sin 3\theta - \frac{(\lambda + \mu)}{2} \frac{\partial_{A2}}{\partial} \rho g r \cos \theta \\ & + \left[ \left\{ (\lambda + 2\mu) \frac{\partial_{A2}}{\partial} - 2\mu \frac{\partial_{C3}}{\partial} \right\} \xi + \left\{ -(\lambda + 2\mu) \frac{\partial_{A1}}{\partial} + 2\mu \frac{\partial_{C4}}{\partial} + 1 \right\} \eta \right] \rho g \cos 2\theta \end{aligned}$$

$$+ \left[ -\frac{(\lambda + 3\mu)}{2} \frac{\partial A_2}{\partial} + 2\mu \frac{\partial C_3}{\partial} \right] \rho g r \cos 3\theta. \dots\dots\dots (41)$$

In the present study the boundary conditions of elasticity are as follows: (Referring to Fig. 3.)

1. On the two surfaces *OY* and *OX* the normal and shearing components of stress are zero.

2. On the surface of the horizontal circular hole, the normal and shearing components of stress are zero.

It is difficult to satisfy these conditions completely, and it is, however, our object to investigate the stress distribution in the vicinity of the hole, and therefore we may take the following conditions instead of of the above two conditions:

1. The stress at the whole space far from the horizontal hole in the wedge-shaped solid is equal to that expressed by (39), (40) and (41).

2. The surface of this hole is completely free from traction.

These are denoted by

$$\left. \begin{aligned} r = \infty; \quad \widehat{rr} = \widehat{rr} \text{ expressed by (39),} \\ \widehat{\theta\theta} = \widehat{\theta\theta} \text{ expressed by (40),} \\ \widehat{r\theta} = \widehat{r\theta} \text{ expressed by (41),} \end{aligned} \right\} \dots\dots\dots (42)$$

$$\left. \begin{aligned} r = a; \quad \widehat{rr} = 0, \\ \widehat{r\theta} = 0. \end{aligned} \right\} \dots\dots\dots (43)$$

Using the expressions of stress, (36), (37) and (38), which are the general solutions of the equilibrium of the solid, and the conditions (42) and (43), we find the values of the arbitrary constants as follows:

From (42);

$$\left. \begin{aligned} B_0 = \rho g \left\{ -\frac{\partial A_1}{\partial} \xi + \frac{\partial A_2}{\partial} \eta \right\}, \quad B_1 = \rho g \frac{\partial A_1}{\partial}, \quad B_3 = 0, \quad D_2 = 0, \quad D_3 = 0. \\ B_2'' = \frac{\rho g}{2\mu} \left[ \left\{ -\mu \frac{\partial A_1}{\partial} + 2\mu \frac{\partial C_4}{\partial} \right\} \xi + \left\{ -\mu \frac{\partial A_2}{\partial} + 2\mu \frac{\partial C_3}{\partial} \right\} \eta \right], \\ B_3'' = \frac{\rho g}{4\mu} \left[ \frac{(\lambda + 3\mu)}{2} \frac{\partial A_1}{\partial} - 2\mu \frac{\partial C_4}{\partial} - \frac{1}{2} \right], \quad D_3'' = \frac{\rho g}{4\mu} \left\{ -\frac{(\lambda + 3\mu)}{2} \frac{\partial A_2}{\partial} + 2\mu \frac{\partial C_3}{\partial} \right\}, \\ D_2'' = \frac{\left[ \left\{ (\lambda + 2\mu) \frac{\partial A_2}{\partial} - 2\mu \frac{\partial C_3}{\partial} \right\} \xi + \left\{ -(\lambda + 2\mu) \frac{\partial A_1}{\partial} + 2\mu \frac{\partial C_4}{\partial} + 1 \right\} \eta \right] \rho g}{2\mu}. \end{aligned} \right\} (44)$$

From (43):—

$$\begin{aligned}
 B_0'' &= -\frac{(\lambda + \mu)}{2\mu} \left\{ \frac{\partial_{A_1}}{\partial} \xi - \frac{\partial_{A_2}}{\partial} \eta \right\} \rho g a^2, \quad F_1 = -\frac{\rho g a^2}{2(\lambda + 2\mu)}, \\
 C_1'' &= \frac{(\lambda + \mu)}{8\mu} \rho g \frac{\partial_{A_1}}{\partial} a^4 - \frac{(\lambda + \mu)}{8\mu(\lambda + 2\mu)} \rho g a^4, \quad E_1 = 0, \\
 E_1'' &= \frac{\rho g(\lambda + \mu)}{8\mu} \frac{\partial_{A_2}}{\partial} a^4, \quad E_2 = -\frac{2\rho g a^2}{(\lambda + \mu)} \\
 &\quad \times \left[ \left\{ (\lambda + 2\mu) \frac{\partial_{A_2}}{\partial} - 2\mu \frac{\partial_{C_3}}{\partial} \right\} \xi + \left\{ -(\lambda + 2\mu) \frac{\partial_{A_1}}{\partial} + 2\mu \frac{\partial_{C_4}}{\partial} + 1 \right\} \eta \right], \\
 E_2'' &= -\frac{\rho g a^4}{2\mu} \left[ \left\{ (\lambda + 2\mu) \frac{\partial_{A_2}}{\partial} - 2\mu \frac{\partial_{C_3}}{\partial} \right\} \xi + \left\{ -(\lambda + 2\mu) \frac{\partial_{A_1}}{\partial} \right. \right. \\
 &\quad \left. \left. + 2\mu \frac{\partial_{C_4}}{\partial} + 1 \right\} \eta \right], \\
 C_3 &= -\frac{2\rho g a^4}{(\lambda + \mu)} \left[ \frac{(\lambda + 3\mu)}{2} \frac{\partial_{A_1}}{\partial} - 2\mu \frac{\partial_{C_4}}{\partial} - \frac{1}{2} \right], \\
 C_3'' &= -\frac{\rho g a^6}{2\mu} \left[ \frac{(\lambda + 3\mu)}{2} \frac{\partial_{A_1}}{\partial} - 2\mu \frac{\partial_{C_4}}{\partial} - \frac{1}{2} \right], \\
 E_3 &= -\frac{2\rho g a^4}{(\lambda + \mu)} \left\{ -\frac{(\lambda + 3\mu)}{2} \frac{\partial_{A_2}}{\partial} + 2\mu \frac{\partial_{C_3}}{\partial} \right\}, \\
 E_3'' &= -\frac{\rho g a^6}{2\mu} \left\{ -\frac{(\lambda + 3\mu)}{2} \frac{\partial_{A_2}}{\partial} + 2\mu \frac{\partial_{C_3}}{\partial} \right\}. \\
 C_2 &= -\frac{2\rho g a^2}{(\lambda + \mu)} \left[ \left\{ -\mu \frac{\partial_{A_1}}{\partial} + 2\mu \frac{\partial_{C_4}}{\partial} \right\} \xi + \left\{ -\mu \frac{\partial_{A_2}}{\partial} + 2\mu \frac{\partial_{C_3}}{\partial} \right\} \eta \right], \\
 C_2'' &= -\frac{\rho g a^4}{2\mu} \left[ \left\{ -\mu \frac{\partial_{A_1}}{\partial} + 2\mu \frac{\partial_{C_4}}{\partial} \right\} \xi + \left\{ -\mu \frac{\partial_{A_2}}{\partial} + 2\mu \frac{\partial_{C_3}}{\partial} \right\} \eta \right].
 \end{aligned} \tag{45}$$

Substituting these values (44) and (45) for  $B_0, B_1, B_3, D_2, D_3, B_2'', B_3'', D_2'', D_3'', B_0'', F_1, C_1'', C_2, C_2'', E_1, E_1'', E_2, E_2'', C_3, C_3'', E_3$  and  $E_3''$  in the expressions (36), (37) and (38), we obtain the final results of the stress which are favourable to the present study as follows:

$$\begin{aligned}
 \widehat{r r} &= (\lambda + \mu) \rho g \left\{ \xi \frac{\partial_{A_1}}{\partial} - \eta \frac{\partial_{A_2}}{\partial} \right\} \left\{ -1 + \frac{a^2}{r^2} \right\} \\
 &\quad + \rho g \left[ \frac{(\lambda + \mu)}{2} \frac{\partial_{A_1}}{\partial} \left( r - \frac{a^4}{r^3} \right) + \frac{1}{2} \left\{ r - \frac{(2\lambda + 3\mu)}{(\lambda + 2\mu)} \frac{a^2}{r} + \frac{(\lambda + \mu)}{(\lambda + 2\mu)} \frac{a^4}{r^3} \right\} \right] \cos \theta \\
 &\quad + \rho g \left[ \left\{ -\mu \frac{\partial_{A_1}}{\partial} + 2\mu \frac{\partial_{C_4}}{\partial} \right\} \xi + \left\{ -\mu \frac{\partial_{A_2}}{\partial} + 2\mu \frac{\partial_{C_3}}{\partial} \right\} \eta \right] \left\{ 1 - \frac{4a^2}{r^2} + \frac{3a^4}{r^4} \right\} \cos 2\theta
 \end{aligned}$$

$$\begin{aligned}
 &+ \rho g \left[ \frac{(\lambda + 3\mu)}{2} \frac{\partial_{A2}}{\partial} - 2\mu \frac{\partial_{C4}}{\partial} - \frac{1}{2} \right] \left\{ r - \frac{5a^4}{r^3} + \frac{4a^6}{r^5} \right\} \cos 3\theta \\
 &+ \rho g \frac{(\lambda + \mu)}{2} \frac{\partial_{A2}}{\partial} \left( r - \frac{a^4}{r^3} \right) \sin \theta \\
 &+ \rho g \left[ \left\{ (\lambda + 2\mu) \frac{\partial_{A2}}{\partial} - 2\mu \frac{\partial_{C3}}{\partial} \right\} \xi + \left\{ -(\lambda + 2\mu) \frac{\partial_{A1}}{\partial} + 2\mu \frac{\partial_{C4}}{\partial} + 1 \right\} \eta \right] \\
 &\quad \times \left\{ 1 - \frac{4a^2}{r^2} + \frac{3a^4}{r^4} \right\} \sin 2\theta \\
 &+ \rho g \left[ -\frac{(\lambda + 3\mu)}{2} \frac{\partial_{A2}}{\partial} + 2\mu \frac{\partial_{C3}}{\partial} \right] \left\{ r - 5 \frac{a^4}{r^3} + 4 \frac{a^6}{r^5} \right\} \sin 3\theta, \dots \dots \dots (46)
 \end{aligned}$$

$$\begin{aligned}
 \widehat{\theta\theta} = & -(\lambda + \mu) \rho g \left\{ \xi \frac{\partial_{A1}}{\partial} - \eta \frac{\partial_{A2}}{\partial} \right\} \left\{ 1 + \frac{a^2}{r^2} \right\} \\
 &+ \rho g \left[ \frac{(\lambda + \mu)}{2} \frac{\partial_{A1}}{\partial} \left( 3r + \frac{a^4}{r^3} \right) + \frac{1}{2} \left\{ -r + \frac{\mu a^2}{(\lambda + 2\mu)r} - \frac{(\lambda + \mu)}{(\lambda + 2\mu)} \frac{a^4}{r^3} \right\} \right] \cos \theta \\
 &+ \rho g \left[ \left\{ \mu \frac{\partial_{A1}}{\partial} - 2\mu \frac{\partial_{C4}}{\partial} \right\} \xi + \left\{ \mu \frac{\partial_{A2}}{\partial} - 2\mu \frac{\partial_{C3}}{\partial} \right\} \eta \right] \left\{ 1 + \frac{3a^4}{r^4} \right\} \cos 2\theta \\
 &+ \rho g \left[ \frac{(\lambda + 3\mu)}{2} \frac{\partial_{A1}}{\partial} - 2\mu \frac{\partial_{C4}}{\partial} - \frac{1}{2} \right] \left\{ -r + \frac{a^4}{r^3} - \frac{4a^6}{r^5} \right\} \cos 3\theta \\
 &+ \frac{(\lambda + \mu)}{2} \rho g \frac{\partial_{A2}}{\partial} \left\{ 3r - \frac{a^4}{r^3} \right\} \sin \theta \\
 &+ \rho g \left[ \left\{ -(\lambda + 2\mu) \frac{\partial_{A2}}{\partial} + 2\mu \frac{\partial_{C3}}{\partial} \right\} \xi + \left\{ (\lambda + 2\mu) \frac{\partial_{A1}}{\partial} - 2\mu \frac{\partial_{C4}}{\partial} - 1 \right\} \eta \right] \\
 &\quad \times \left\{ 1 + \frac{3a^4}{r^4} \right\} \sin 2\theta \\
 &+ \rho g \left[ -\frac{(\lambda + 3\mu)}{2} \frac{\partial_{A2}}{\partial} + 2\mu \frac{\partial_{C3}}{\partial} \right] \left\{ -r + \frac{a^4}{r^3} - 4 \frac{a^6}{r^5} \right\} \sin 3\theta, \dots \dots \dots (47)
 \end{aligned}$$

$$\begin{aligned}
 \widehat{r\theta} = & \rho g \left[ \frac{(\lambda + \mu)}{2} \frac{\partial_{A1}}{\partial} \left\{ r - \frac{a^4}{r^3} \right\} + \frac{1}{2} \left\{ -r + \frac{\mu}{(\lambda + 2\mu)} \frac{a^2}{r} + \frac{(\lambda + \mu)}{(\lambda + 2\mu)} \frac{a^4}{r^3} \right\} \right] \sin \theta \\
 &+ \rho g \left[ \left\{ -\mu \frac{\partial_{A1}}{\partial} + 2\mu \frac{\partial_{C4}}{\partial} \right\} \xi + \left\{ -\mu \frac{\partial_{A2}}{\partial} + 2\mu \frac{\partial_{C3}}{\partial} \right\} \eta \right]
 \end{aligned}$$

$$\begin{aligned}
 & \times \left\{ -1 - \frac{2a^2}{r^2} + \frac{3a^4}{r^4} \right\} \sin 2\theta \\
 & + \rho g \left[ \frac{(\lambda + 3\mu)}{2} \frac{\partial_{A1}}{\partial} - 2\mu \frac{\partial_{C4}}{\partial} - \frac{1}{2} \right] \left\{ -r - \frac{3a^4}{r^3} + \frac{4a^6}{r^5} \right\} \sin 3\theta \\
 & - \rho g \frac{(\lambda + \mu)}{2} \frac{\partial_{A2}}{\partial} \left\{ r - \frac{a^4}{r^3} \right\} \cos \theta \\
 & + \rho g \left[ \left\{ (\lambda + 2\mu) \frac{\partial_{A2}}{\partial} - 2\mu \frac{\partial_{C3}}{\partial} \right\} \xi + \left\{ -(\lambda + 2\mu) \frac{\partial_{A1}}{\partial} + 2\mu \frac{\partial_{C4}}{\partial} + 1 \right\} \eta \right] \\
 & \quad \times \left\{ 1 + \frac{2a^2}{r^2} - \frac{3a^4}{r^4} \right\} \cos 2\theta \\
 & + \rho g \left[ -\frac{(\lambda + 3\mu)}{2} \frac{\partial_{A2}}{\partial} + 2\mu \frac{\partial_{C3}}{\partial} \right] \left\{ r + 3\frac{a^4}{r^3} - 4\frac{a^6}{r^5} \right\} \cos 3\theta. \dots\dots\dots(48)
 \end{aligned}$$

As  $\widehat{\theta}_{r=a}$  on the surface of the hole play an important rôle on the failure of the tunnel, it may be of some importance to investigate the properties of the stress distribution around the surface of the horizontal hole. For this purpose we assume  $\lambda = \mu$  (Poisson's ratio = 1/4). Then the tangential stress  $\widehat{\theta}_{r=a}$  on the surface of the hole is expressed by the following simplified form:

$$\widehat{\theta}_{r=a} = \theta + \Phi + \Psi, \dots\dots\dots(49)$$

where

$$\frac{\theta}{\rho g a} = \left( 4 \frac{\partial_{A1}}{\partial} - \frac{2}{3} \right) \cos \theta - 4 \left\{ 4 \frac{\partial_{A1}}{\partial} - 4 \frac{\partial_{C4}}{\partial} - 1 \right\} \cos 3\theta - 8 \frac{\partial_{C3}}{\partial} \sin 3\theta, (50)$$

$$\frac{\Phi}{\rho g a} = -4 \frac{\partial_{A1}}{\partial} + 4 \left\{ \frac{\partial_{A1}}{\partial} - 2 \frac{\partial_{C4}}{\partial} \right\} \cos 2\theta + 8 \frac{\partial_{C3}}{\partial} \sin 2\theta, \dots\dots\dots(51)$$

$$\frac{\Psi}{\rho g a} = -8 \frac{\partial_{C3}}{\partial} \cos 2\theta + 4 \left\{ 3 \frac{\partial_{A1}}{\partial} - 2 \frac{\partial_{C4}}{\partial} - 1 \right\} \sin 2\theta. \dots\dots\dots(52)$$

Substituting the relations in Table I for the expressions of  $\frac{\partial_{A1}}{\partial}$ ,  $\frac{\partial_{A2}}{\partial}$ ,  $\frac{\partial_{C3}}{\partial}$  and  $\frac{\partial_{C4}}{\partial}$  in the right-hand terms of  $\theta$ ,  $\Phi$ ,  $\Psi$ , we obtain Table III in which  $\theta$ ,  $\Phi$ , and  $\Psi$  expressed by terms  $\theta$  only are tabulated in the cases of  $\varphi = 0^\circ, 20^\circ, 30^\circ, 45^\circ, 60^\circ$  and  $70^\circ$ .



Table III.

$\varphi$	$0^\circ$	$20^\circ$	$30^\circ$	$45^\circ$	$60^\circ$	$70^\circ$
$\theta$	$\frac{1}{3} \cos \theta$ $-\cos 3\theta$	$\frac{1}{3} \cos \theta$ $-0.175 \cos 3\theta$ $-0.984 \sin 3\theta$	$\frac{1}{3} \cos \theta$ $+0.496 \cos 3\theta$ $-0.864 \sin 3\theta$	$\frac{1}{3} \cos \theta$ $+\cos 3\theta$	$\frac{1}{3} \cos \theta$ $+0.496 \cos 3\theta$ $+0.864 \sin 3\theta$	$\frac{1}{3} \cos \theta$ $-0.175 \cos 3\theta$ $+0.984 \sin 3\theta$
$\Phi$	$-1$ $+2\cos 2\theta$	$-1$ $+1.175 \cos 2\theta$ $+0.984 \sin 2\theta$	$-1$ $+0.504 \cos 2\theta$ $+0.864 \sin 2\theta$	$-1$	$-1$ $+0.504 \cos 2\theta$ $-0.864 \sin 2\theta$	$-1$ $+1.175 \cos 2\theta$ $-0.984 \sin 2\theta$
$\Psi$	$0$	$-0.984 \cos 2\theta$ $-0.825 \sin 2\theta$	$-0.864 \cos 2\theta$ $-1.496 \sin 2\theta$	$-2$ $\times \sin 2\theta$	$0.864 \cos 2\theta$ $-1.496 \sin 2\theta$	$0.984 \cos 2\theta$ $-0.825 \sin 2\theta$

The magnitudes  $\theta$ ,  $\Phi$  and  $\Psi$  in Table III are easily calculated, and the results are tabulated in Table IV, V, and VI, and illustrated in Fig. 5, 6, 7, 8, 9, 10, 11, 12, 13, 14, 15, 16, 17, 18, 19, 20, 21.

The following properties may be seen from these tables and figures :

1. When  $\varphi=0^\circ$  and  $45^\circ$ , the distribution of  $\theta$  and  $\Phi$  are symmetrical about the axis  $o'x'$  (vertical axis).  $\Phi$  has especially a constant value ( $-\rho g \xi$ ) uniformly distributed on the surface of the hole in the case of  $\varphi=45^\circ$ .

2. The curves denoting  $\Phi$  and  $\Psi$  have regular forms of certain constant amplitudes of fluctuation for different  $\theta$ , and their mean lines are the lines of  $\Phi=-\rho g \xi$  and  $\Psi=0$  respectively in all cases of  $\varphi$ . The curve denoting  $\theta$ , however, has irregular amplitudes.

3. The amplitudes of the curves of  $\Phi$  and  $\Psi$  are variable according to the magnitude of  $\varphi$ . The curve denoting  $\Phi$  has the largest amplitude when  $\varphi=0^\circ$  or  $90^\circ$ ; and the amplitude of  $\Psi$  takes the largest value when  $\varphi=45^\circ$ .

4. The positions of maxima and minima of the amplitudes of  $\theta$ ,  $\Phi$ ,  $\Psi$  shift regularly and systematically along  $\theta$ -axis between  $\theta=0^\circ$  and  $\theta=360^\circ$  according to the variation of  $\varphi$  between 0 and  $90^\circ$ .

5.  $\Psi$  has no effect upon the stress distribution when  $\varphi=0$ . When  $\varphi=45^\circ$ ,  $\Psi$  takes the largest values  $200 \rho g \eta$  (with positive sign) at  $\theta=135^\circ$  and  $\theta=315^\circ$ , and also similar values (with negative sign) at  $\theta=45^\circ$  and  $225^\circ$ .

Next we shall study the numerical variation of  $\widehat{\theta\theta}_{r=\alpha}$  according to different values of  $\xi$ ,  $\eta$  and  $\varphi$ . Before entering this investigation, the

Table IV. (Magnitude of  $\frac{\theta}{\rho g a}$ .)

$\varphi$ $\theta$	0°	20°	30°	45°	60°	70°
0°	-0.67	0.16	0.83	1.33	0.83	0.16
10	-0.54	-0.32	0.24	1.19	1.19	0.67
20	-0.19	-0.63	-0.24	0.81	1.31	1.08
30	0.29	-0.70	-0.58	0.29	1.15	1.27
45	0.94	-0.34	-0.65	-0.47	0.50	1.06
60	1.17	0.34	-0.33	-0.83	-0.33	0.34
70	0.98	0.76	0.20	-0.75	-0.75	-0.23
80	0.56	1.00	0.61	-0.44	-0.94	-0.71
90	0	0.98	0.86	0	-0.86	-0.98
100	-0.56	0.71	0.89	0.44	-0.56	-1.00
110	-0.98	0.22	0.66	0.75	-0.12	-0.76
120	-1.17	-0.34	0.33	0.83	0.33	-0.34
135	-0.94	-1.05	-0.57	0.47	0.72	0.34
150	-0.29	-1.27	-1.15	-0.29	0.58	0.70
160	0.19	-1.08	-1.26	-0.81	0.19	0.63
170	0.54	-0.66	-1.10	-1.19	-0.33	0.32
180	0.67	-0.16	-0.83	-1.33	-0.83	-0.16
190	0.54	0.32	-0.24	-1.19	-1.19	-0.67
200	0.19	0.63	0.24	-0.81	-1.31	-1.08
210	-0.29	0.70	0.58	-0.29	-1.15	-1.27
225	-0.94	0.34	0.65	0.47	-0.50	-1.06
240	-1.17	-0.34	0.33	0.83	0.33	-0.34
250	-0.98	-0.76	-0.20	0.75	0.75	0.23
260	-0.56	-1.00	-0.61	0.44	0.94	0.71
270	0	-0.98	-0.86	0	0.86	0.98
280	0.56	-0.71	-0.89	-0.44	0.56	1.00
290	0.98	-0.22	-0.66	-0.75	0.12	0.76
300	1.17	0.34	-0.33	-0.83	-0.33	0.34
315	0.94	1.05	0.57	-0.47	-0.72	-0.34
330	0.29	1.27	1.15	0.29	-0.58	-0.70
340	-0.19	1.08	1.26	0.81	-0.19	-0.63
350	-0.54	0.66	1.10	1.19	0.33	-0.32
360	-0.67	0.16	0.83	1.33	0.83	0.16

Table V. (Magnitude of  $\frac{\Phi}{\rho g \xi}$ .)

$\theta \backslash \varphi$	0°	20°	30°	45°	60°	70°
0°	1.00	0.18	-0.50	-1	-0.50	0.18
10	0.88	0.44	-0.23	-1	-0.82	-0.24
20	0.53	0.53	-0.06	-1	-1.17	-0.73
30	0	0.44	0	-1	-1.50	-1.27
45	-1.00	-0.02	-0.14	-1	-1.86	-1.98
60	-2.00	-0.74	-0.50	-1	-2.00	-2.44
70	-2.53	-1.27	-0.83	-1	-1.94	-2.53
80	-2.88	-1.77	-1.18	-1	-1.77	-2.44
90	-3.00	-2.18	-1.50	-1	-1.50	-2.18
100	-2.88	-2.44	-1.77	-1	-1.18	-1.76
110	-2.53	-2.53	-1.94	-1	-0.83	-1.27
120	-2.00	-2.44	-2.00	-1	-0.50	-0.73
135	-1.00	-1.98	-1.86	-1	-0.14	-0.02
150	0	-1.27	-1.50	-1	0	0.44
160	0.53	-0.73	-1.17	-1	-0.06	0.53
170	0.87	-0.23	-0.82	-1	-0.23	0.44
180	1.00	0.18	-0.50	-1	-0.50	0.18
190	0.87	0.44	-0.23	-1	-0.82	-0.24
200	0.53	0.53	-0.06	-1	-1.17	-0.73
210	0	0.44	0	-1	-1.50	-1.27
225	-1.00	-0.02	-0.14	-1	-1.86	-1.98
240	-2.00	-0.74	-0.50	-1	-2.00	-2.44
250	-2.53	-1.27	-0.83	-1	-1.94	-2.53
260	-2.88	-1.77	-1.18	-1	-1.77	-2.44
270	-3.00	-2.18	-1.50	-1	-1.50	-2.18
280	-2.88	-2.44	-1.77	-1	-1.18	-1.76
290	-2.53	-2.53	-1.94	-1	-0.83	-1.27
300	-2.00	-2.44	-2.00	-1	-0.50	-0.73
315	-1.00	-1.98	-1.86	-1	-0.14	-0.02
330	0	-1.27	-1.50	-1	0	0.44
340	0.53	-0.73	-1.17	-1	-0.06	0.53
350	0.88	-0.23	-0.82	-1	-0.23	0.44
360	1.00	0.18	-0.50	-1	-0.50	0.18

Table VI. (Magnitude of  $\frac{Y}{\rho g \eta}$ .)

$\varphi$ $\theta$	0°	20°	30°	45°	60°	70°
6°	0	-0.98	-0.86	0	0.86	0.98
10	"	-1.21	-1.32	-0.68	0.30	0.64
20	"	-1.29	-1.62	-1.29	-0.30	0.22
30	"	-1.21	-1.72	-1.73	-0.86	-0.22
45	"	-0.83	-1.50	-2.00	-1.50	-0.83
60	"	0.23	-0.86	-1.73	-1.73	-1.21
70	"	0.23	-0.30	-1.29	-1.62	-1.28
80	"	0.64	0.30	-0.68	-1.32	-1.21
90	"	0.98	0.86	0	-0.86	-0.98
100	"	1.21	1.32	0.68	-0.30	-0.64
110	"	1.29	1.62	1.29	0.30	-0.22
120	"	1.21	1.72	1.73	0.86	0.22
135	"	0.83	1.50	2.00	1.50	0.83
150	"	0.22	0.86	1.73	1.73	1.21
160	"	-0.23	0.30	1.29	1.62	1.28
170	"	-0.64	-0.30	0.68	1.32	1.21
180	"	-0.98	-0.86	0	0.86	0.98
190	"	-1.21	-1.32	-0.68	0.30	0.64
200	"	-1.29	-1.62	-1.29	-0.30	0.22
210	"	-1.21	-1.72	-1.73	-0.86	-0.22
225	"	-0.83	-1.50	-2.00	-1.50	-0.83
240	"	-0.22	-0.86	-1.73	-1.73	-1.21
250	"	0.23	-0.30	-1.29	-1.62	-1.28
260	"	0.64	0.30	-0.68	-1.32	-1.21
270	"	0.98	0.86	0	-0.86	-0.98
280	"	1.21	1.32	0.68	-0.30	-0.64
290	"	1.29	1.62	1.29	0.30	-0.22
300	"	1.21	1.72	1.73	0.86	0.22
315	"	0.83	1.50	2.00	1.50	0.83
330	"	0.23	0.86	1.73	1.73	1.21
340	"	-0.23	0.30	1.29	1.62	1.28
350	"	-0.64	-0.30	0.68	1.32	1.21
360	"	-0.98	-0.86	0	0.86	0.98

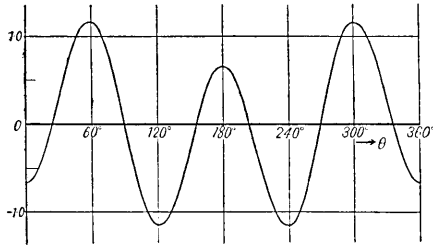


Fig. 5. Magnitude of  $\frac{\theta}{\rho ga}$  when  $\varphi = 0$ .

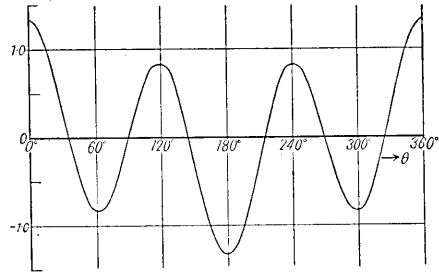


Fig. 8. Magnitude of  $\frac{\theta}{\rho ga}$  when  $\varphi = 45^\circ$ .

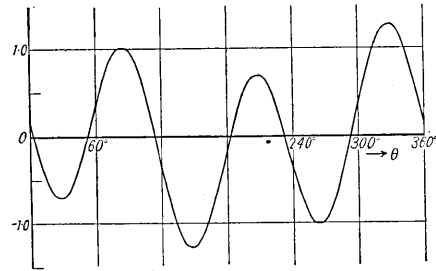


Fig. 6. Magnitude of  $\frac{\theta}{\rho ga}$  when  $\varphi = 20^\circ$ .

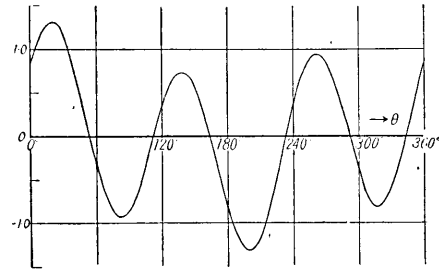


Fig. 9. Magnitude of  $\frac{\theta}{\rho ga}$  when  $\varphi = 60^\circ$ .

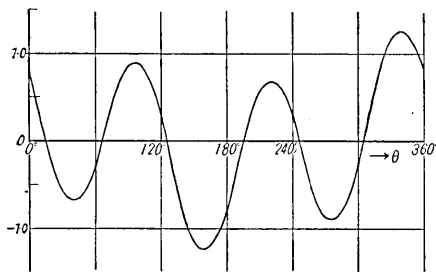


Fig. 7. Magnitude of  $\frac{\theta}{\rho ga}$  when  $\varphi = 30^\circ$ .

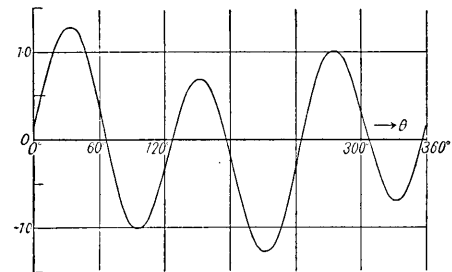


Fig. 10. Magnitude of  $\frac{\theta}{\rho ga}$  when  $\varphi = 70^\circ$ .

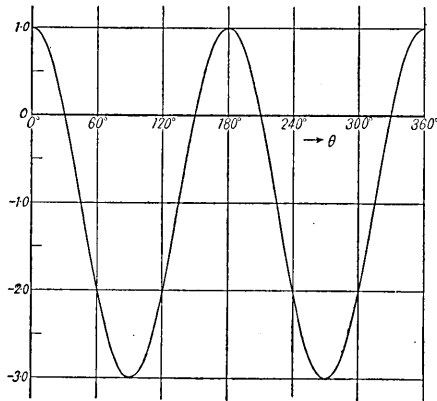


Fig. 11. Magnitude of  $\frac{\bar{\Phi}}{\rho g \xi}$  when  $\varphi = 0^\circ$ .

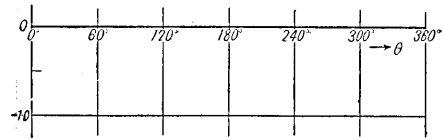


Fig. 14. Magnitude of  $\frac{\bar{\Phi}}{\rho g \xi}$  when  $\varphi = 45^\circ$ .

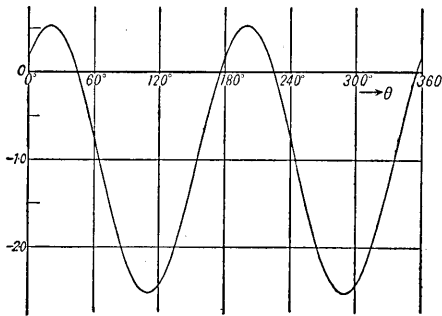


Fig. 12. Magnitude of  $\frac{\bar{\Phi}}{\rho g \xi}$  when  $\varphi = 20^\circ$ .

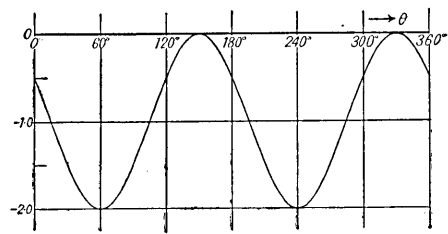


Fig. 15. Magnitude of  $\frac{\bar{\Phi}}{\rho g \xi}$  when  $\varphi = 60^\circ$ .

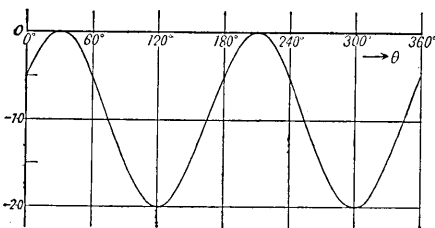


Fig. 13. Magnitude of  $\frac{\bar{\Phi}}{\rho g \xi}$  when  $\varphi = 30^\circ$ .

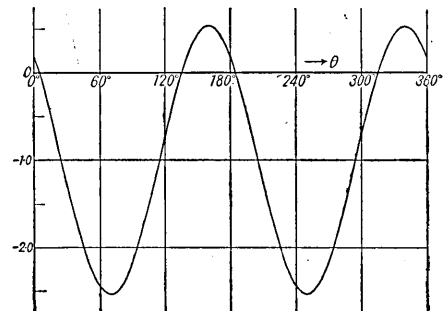


Fig. 16. Magnitude of  $\frac{\bar{\Phi}}{\rho g \xi}$  when  $\varphi = 70^\circ$ .

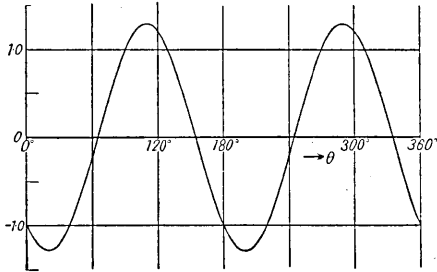


Fig. 17. Magnitude of  $\frac{\psi}{\rho g \eta}$  when  $\varphi = 20^\circ$ .

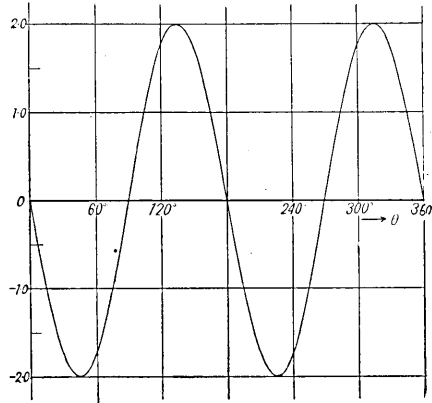


Fig. 19. Magnitude of  $\frac{\psi}{\rho g \eta}$  when  $\varphi = 45^\circ$ .

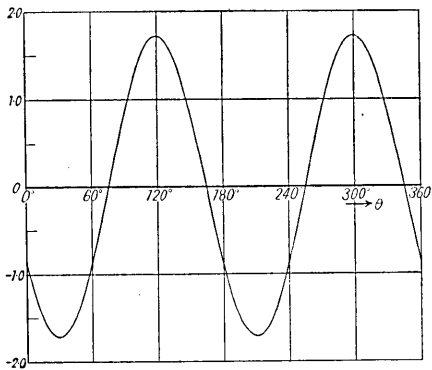


Fig. 18. Magnitude of  $\frac{\psi}{\rho g \eta}$  when  $\varphi = 30^\circ$ .

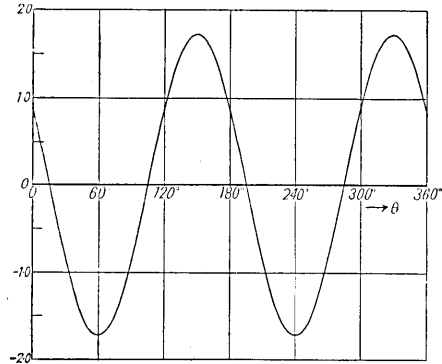


Fig. 20. Magnitude of  $\frac{\psi}{\rho g \eta}$  when  $\varphi = 60^\circ$ .

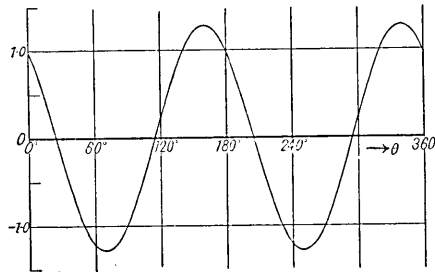


Fig. 21. Magnitude of  $\frac{\psi}{\rho g \eta}$  when  $\varphi = 70^\circ$ .

short notice will be given. We can easily obtain the following relation :

$$\xi = \{m \operatorname{cosec} \varphi + \eta\} \tan \varphi, \dots \dots \dots (53)$$

where  $m$  is the minimum distance from the centre of the hole to the surface of the wedge-shaped solid  $OY$ . The elasticity conditions of the present study are of the expressions of (42) and (43), and therefore  $m$  and  $\xi$  should be larger than the radius of the hole  $a$ .

Using Table IV, V, VI relating to  $\theta$ ,  $\Phi$  and  $\Psi$  and the expressions (49), we obtained the numerical values of  $\theta\theta_{r=a}$  in various cases of  $\varphi$ ,  $\xi$  and  $\eta$ . The results thus derived are tabulated in the annexed tables (Table VIII~XXIII), and are shewn in the annexed figures (Fig. 22~37). The magnitudes of  $\varphi$ ,  $\xi$  and  $\eta$  of which we treated in these tables and figures are tabulated in the following table, for the convenience sake. (Table VII.)

Table VII.

Table No.	Fig. No.	$\varphi$ in degree	$\frac{\xi}{a}$	$\frac{\eta}{a}$
VIII	22	0	10	
	23	0	15	
	24	0	20	
IX	25	20°	10	0, 2, 4, 6, 10, 15, 20
X	26	20°	15	0, 2, 4, 6, 10, 15, 20
XI	27	20°	20	0, 2, 4, 6, 10, 15, 20, 25, 30
XII	28	30°	10	0, 2, 4, 6, 10, 13
XIII	29	30°	15	0, 2, 4, 6, 10, 13, 20
XIV	30	30°	20	0, 2, 4, 6, 10, 13, 15, 20, 25
XV	31	45°	10	0, 2, 4, 6, 7.5
XVI	32	45°	15	0, 2, 4, 6, 7.5
XVII	33	45°	20	0, 2, 4, 6, 10, 15
XVIII	34	60°	10	0, 2, 3.5
XIX	35	60°	15	0, 2, 3.5
XX	36	60°	20	0, 2, 6, 8
XXI	37	70°	10	0, 2
XXII		70°	15	0, 2, 4
XXIII		70°	20	0, 2, 4, 6



These tables and figures shew us many interesting properties related to  $\widehat{\theta\theta}_{r=a}$ , and some of them are summarized as follows :

1)  $\varphi=0$  :—

a.  $\widehat{\theta\theta}_{r=a}$  has a distribution symmetrical about the vertical axis passing through the centre of the hole.

b. The magnitude of  $\frac{\eta}{a}$  has no effect upon the stress distribution.

c. The stresses at the top and the bottom of the hole are tensile, but their magnitudes are less than that of the compressive stresses at  $\theta=90^\circ$  and  $270^\circ$ .

2)  $\varphi=20^\circ$  :—

a. The distribution of  $\widehat{\theta\theta}_{r=a}$  is completely different from that in the case of  $\varphi=0$  and it is much affected by the variation of  $\frac{\eta}{a}$ .

b. When  $\frac{\eta}{a}$  is zero, the maxima of tensile stresses occur at  $\theta=20^\circ$  and  $200^\circ$ , and that of compressive stresses at  $\theta=110^\circ$  and  $290^\circ$ . And the latter is larger than the former.

c. The magnitudes of stresses at all points, excepting the points  $\theta=65^\circ, 155^\circ, 245^\circ$  and  $335^\circ$  vary with the increase of  $\frac{\eta}{a}$ , and at certain values of  $\frac{\eta}{a}$  the signs of stresses at some positions change. In the cases of  $(\frac{\xi}{a}=10, \frac{\eta}{a}=6)$ ,  $(\frac{\xi}{a}=15, \frac{\eta}{a}=10)$  and  $(\frac{\xi}{a}=20, \frac{\eta}{a}=10)$  the stresses in the vicinity of  $\theta=200^\circ$  are compressive, while the stresses in the cases of  $(\frac{\xi}{a}=10, \frac{\eta}{a}=0)$ ,  $(\frac{\xi}{a}=15, \frac{\eta}{a}=0)$  and  $(\frac{\xi}{a}=20, \frac{\eta}{a}=0)$  are tensile.

d.  $\widehat{\theta\theta}_{r=a}$  increases linearly with the increase of  $\frac{\xi}{a}$ , but the rate of this linear increase is different at different point on the surface of the hole. Fig. 38 indicates us these properties. In this figure the case of  $\varphi=20^\circ$  and  $\frac{\eta}{a}=20$  is plotted. (These properties may be seen in all cases of  $\varphi$ .)

3)  $\varphi=45^\circ$  :—

a. When  $\frac{\eta}{a}=0$ , the stresses are of

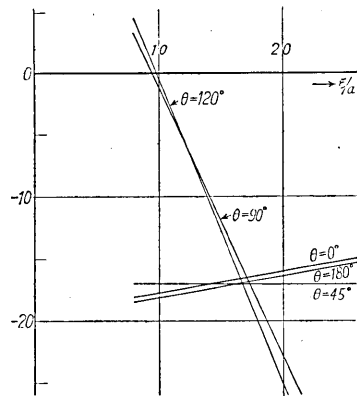


Fig. 38. Magnitude of  $\frac{\theta\theta_{r=a}}{\rho g a}$  when  $\varphi=20^\circ$  and  $\frac{\eta}{a}=20$ .

course distributed symmetrically about the vertical plane passing through the centre of the hole.

b. When  $\frac{\eta}{a}=0$ , the stresses are compressive, and they have no remarkable variations of the distribution as in the case of  $\varphi=0$ .

c. Of course, the positions of maximum and minimum magnitudes of stresses are different from that in the cases of  $\varphi=20^\circ$  and  $30^\circ$ .

3. We have now studied the stress distribution in the neighbourhood of a horizontal circular hole in a gravitating wedge-shaped solid, and may resume some results obtained from the calculations :

1. The maximum values of tension and compression are different in each case of  $\varphi$ , and their positions are also different.

2. The variations of  $\frac{\xi}{a}$  and  $\frac{\eta}{a}$  give no effect upon the variations of the positions of the maxima and minima of the stresses.

3. According to the variation of  $\frac{\eta}{a}$  the sign of stress may change.

4. There are some positions on the surface of the hole where the values of stress do not change in spite of the variation of  $\frac{\eta}{a}$ .

5. The magnitude of stress at a point on the surface of the hole is proportional to the depth of the centre of the hole from the vertex of the solid.

6. The rate of the linear increase of the stress with the depth of the hole is different at different point on the surface of the hole.

In conclusion, the authors must express their sincere thanks to Professor K. Sezawa for his kind guidance.

Table VIII. (Magnitude of  $\frac{\partial\theta_{r=a}}{\rho ga}$  when  $\varphi=0^\circ$ .)

$\theta \backslash \xi/a$	10	15	20	$\theta \backslash \xi/a$	10	15	20
$0^\circ$	9.3	14.3	19.3	190	9.2	13.8	17.9
10	8.3	12.8	17.1	200	5.5	8.2	10.8
20	5.1	7.8	10.4	210	-0.3	-0.3	-0.3
30	0.3	0.3	0.3	225	-10.9	-15.9	-20.9
45	-9.1	-14.1	-19.1	240	-21.2	-31.2	-41.2
60	-18.8	-28.8	-38.8	250	-26.3	-39.0	-51.6
70	-24.3	-37.0	-49.6	260	-29.4	-43.8	-58.2
80	-28.2	-42.7	-57.0	270	-30.0	-45.0	-60.0
90	-30.0	-45.0	-60.0	280	-28.2	-42.6	-57.0
100	-29.4	-43.8	-58.2	290	-24.3	-37.0	-49.6
110	-26.3	-39.0	-51.6	300	-18.8	-28.8	-38.8
120	-21.2	-31.2	-41.2	315	-9.1	-14.1	-19.1
135	-10.9	-15.9	-20.9	330	0.3	0.3	0.3
150	-0.3	-0.3	-0.3	340	5.1	7.8	10.4
160	5.5	8.2	10.8	350	8.3	12.8	17.1
170	9.2	13.8	17.9	360	9.3	14.3	19.3
180	10.7	15.7	20.7				

Table IX. (Magnitude of  $\frac{\widehat{\theta\theta}_{r=a}}{\rho g a}$  when  $\varphi=20^\circ$  and  $\frac{\xi}{a}=10$ .)

$\theta \backslash \eta/a$	0	2	4	6	10	15	20
0°	2.0	0	-1.9	-3.9	-7.8	-12.8	-17.7
10	4.1	1.7	-0.7	-3.2	-8.1	-14.0	-20.0
20.	4.7	2.2	-0.5	-3.0	-8.2	-14.6	-21.0
30	3.7	1.3	-1.1	-3.6	-8.4	-14.4	-20.4
45	-0.5	-2.2	-3.8	-5.5	-8.8	-12.9	-17.0
60	-7.1	-7.6	-8.0	-8.5	-9.4	-10.6	-11.8
70	-11.9	-11.5	-11.0	-10.5	-9.6	-8.5	-7.4
80	-16.7	-15.4	-14.1	-12.8	-10.3	-7.1	-3.8
90	-20.8	-18.8	-16.9	-14.9	-11.0	-6.0	-1.1
100	-23.7	-21.7	-18.9	-16.4	-11.6	-5.6	0.4
110	-25.1	-22.5	-19.9	-17.4	-12.2	-5.8	0.6
120	-24.7	-22.4	-19.9	-17.4	-12.6	-6.6	-0.6
135	-20.9	-19.2	-17.6	-15.9	-12.6	-8.5	-4.4
150	-14.0	-13.6	-13.1	-12.6	-11.8	-10.5	-9.3
160	-8.4	-8.9	-9.3	-9.8	-10.7	-11.8	-12.9
170	-2.9	-4.3	-5.5	-6.8	-9.3	-12.5	-15.8
180	1.6	0	-2.3	-4.3	-8.2	-13.2	-18.1
190	4.7	2.3	-0.1	-2.6	-7.4	-13.4	-19.4
200	5.9	3.3	0.7	-1.8	-7.0	-13.4	-19.8
210	5.1	2.7	0.3	-2.2	-7.0	-13.0	-19.0
225	0.1	-1.6	-3.2	-4.9	-8.2	-12.3	-16.4
240	-7.7	-8.1	-8.6	-9.1	-9.9	-11.2	-12.4
250	-13.5	-13.0	-12.6	-12.1	-11.2	-10.1	-9.0
260	-18.7	-17.4	-16.1	-14.8	-12.3	-9.1	-5.8
270	-22.8	-20.9	-18.9	-16.9	-13.0	-8.0	-3.1
280	-25.1	-22.7	-20.3	-17.8	-13.0	-7.0	-1.0
290	-25.5	-22.9	-20.3	-17.8	-12.6	-6.2	0.2
300	-24.1	-21.7	-19.3	-16.8	-12.0	-6.0	0
315	-18.7	-17.1	-15.4	-13.7	-10.4	-6.3	-2.2
330	-11.4	-10.9	-10.5	-10.0	-9.2	-7.9	-6.7
340	-7.2	-6.7	-8.1	-8.6	-9.5	-10.6	-11.7
350	-1.7	-2.9	-4.3	-5.6	-8.1	-11.3	-14.6
360	2.0	0	-1.9	-3.9	-7.8	-12.8	-17.7

Table X. (Magnitude of  $\frac{\widehat{\theta\theta}_{r=a}}{\rho g a}$  when  $\varphi=20^\circ$  and  $\frac{\xi}{a}=15$ .)

$\eta/a$ $\theta$	0	2	4	6	10	15	20	25
0°	2.8	0.8	-1.1	-3.1	-7.0	-12.0	-16.9	-21.8
10	6.3	3.9	1.5	-1.0	-5.8	-11.8	-17.8	-23.9
20	7.4	4.8	2.2	-0.3	-5.5	-11.9	-18.3	-24.8
30	5.9	3.8	1.2	-1.4	-6.2	-12.3	-18.2	-24.3
45	-0.5	-2.2	-3.8	-5.5	-8.8	-12.9	-17.0	-21.1
60	-10.7	-11.2	-11.6	-12.1	-13.0	-14.2	-15.4	-16.5
70	-18.2	-17.7	-17.3	-16.8	-15.9	-14.8	-13.7	-12.7
80	-25.5	-24.2	-22.9	-21.6	-19.1	-15.9	-12.6	-9.4
90	-31.6	-29.6	-27.7	-25.7	-21.8	-16.8	-11.9	-7.0
100	-35.9	-33.5	-31.1	-28.6	-23.8	-17.8	-11.8	-5.7
110	-37.8	-35.2	-32.6	-30.1	-24.9	-18.5	-12.1	-5.6
120	-36.9	-34.5	-32.1	-29.6	-24.8	-18.8	-12.8	-6.7
135	-30.9	-29.2	-27.6	-25.9	-22.6	-18.5	-14.4	-10.3
150	-20.3	-19.8	-19.4	-18.9	-18.0	-16.8	-15.6	-14.5
160	-12.1	-12.6	-13.0	-13.5	-14.4	-15.5	-16.8	-17.6
170	-4.1	-5.4	-6.7	-8.0	-10.5	-13.7	-17.0	-20.2
180	2.4	0.4	-1.5	-3.5	-7.4	-12.4	-17.3	-22.2
190	6.9	4.5	2.1	-0.4	-5.2	-11.2	-17.2	-23.0
200	8.6	6.0	3.4	0.9	-4.3	-10.7	-17.1	-23.6
210	7.3	4.9	2.5	0	-4.8	-10.8	-16.8	-22.9
225	0.1	-1.2	-3.2	-4.9	-8.2	-12.3	-16.4	-20.5
240	-11.3	-11.8	-12.2	-12.7	-13.5	-14.8	-16.0	-17.1
250	-19.8	-19.3	-18.9	-18.4	-17.5	-16.4	-15.3	-14.3
260	-27.5	-26.2	-24.9	-23.6	-21.1	-17.9	-14.6	-11.4
270	-33.6	-31.6	-29.7	-27.7	-23.8	-18.8	-13.9	-9.0
280	-37.3	-34.9	-32.5	-30.0	-25.2	-19.2	-13.2	-7.1
290	-38.2	-35.6	-33.0	-30.5	-25.3	-18.9	-12.5	-6.0
300	-36.3	-33.9	-31.5	-29.0	-24.2	-18.2	-12.2	-6.1
315	-28.7	-27.1	-25.4	-23.7	-20.4	-16.3	-12.2	-8.1
330	-17.7	-17.2	-16.8	-16.3	-15.5	-14.2	-13.0	-11.9
340	-9.9	-10.4	-10.8	-11.3	-12.2	-13.3	-14.4	-15.4
350	-2.8	-4.1	-5.4	-6.7	-9.2	-12.4	-15.7	-18.9
360	2.8	0.8	-1.1	-3.1	-7.0	-12.0	-16.9	-21.8

Table XI. (Magnitude of  $\frac{\widehat{\theta\theta}_{r=a}}{\rho ga}$  when  $\varphi=20^\circ$  and  $\frac{\xi}{a}=20$ .)

$\eta/a$ $\theta$	0	2	4	6	10	15	20	25	30
0°	3.7	1.7	-0.2	-2.2	-6.1	-11.1	-16.0	-20.9	-25.8
10	8.5	6.1	3.7	1.2	-3.6	-9.6	-15.6	-21.7	-27.7
20	10.1	7.5	4.9	2.4	-2.8	-9.2	-15.6	-22.1	-28.5
30	8.1	5.6	3.3	0.8	-4.0	-10.0	-16.0	-22.1	-28.1
45	-0.6	-2.3	-3.9	-5.6	-8.9	-13.0	-17.1	-21.2	-25.4
60	-14.4	-14.9	-15.3	-15.8	-16.7	-17.9	-19.1	-20.2	-21.4
70	-24.5	-24.0	-23.6	-23.1	-22.2	-21.1	-20.0	-19.0	-17.7
80	-34.3	-33.0	-31.7	-30.4	-27.9	-24.7	-21.4	-18.2	-15.0
90	-42.5	-40.5	-38.6	-36.6	-32.7	-27.7	-22.8	-17.9	-13.0
100	-48.1	-45.7	-43.3	-40.8	-36.0	-30.0	-24.0	-17.9	-11.9
110	-50.5	-47.9	-45.3	-42.8	-37.6	-31.2	-24.8	-18.3	-12.3
120	-49.1	-46.7	-44.3	-41.8	-37.0	-31.0	-25.0	-18.9	-12.9
135	-40.8	-39.1	-37.5	-35.8	-32.5	-28.4	-24.3	-20.2	-16.0
150	-26.6	-26.1	-25.7	-25.2	-24.4	-23.1	-21.9	-20.8	-19.6
160	-15.6	-16.1	-16.5	-17.0	-17.9	-19.0	-20.1	-21.1	-22.4
170	-5.3	-6.5	-7.9	-9.2	-11.7	-14.9	-18.2	-21.4	-24.6
180	3.3	1.3	-0.6	-2.6	-6.5	-11.5	-16.4	-21.3	-26.2
190	9.1	6.7	4.3	1.8	-3.0	-9.0	-15.0	-21.1	-27.1
200	11.2	8.6	6.0	3.5	-1.7	-8.1	-14.5	-21.0	-27.0
210	9.5	7.1	4.7	2.2	-2.6	-8.6	-14.6	-20.7	-26.7
225	-0.1	-1.8	-3.4	-5.1	-8.4	-12.5	-16.6	-20.7	-24.9
240	-15.0	-15.5	-15.9	-16.4	-17.2	-18.5	-19.7	-20.8	-22.0
250	-26.0	-25.5	-26.9	-24.6	-23.7	-22.6	-21.5	-20.5	-19.2
260	-36.2	-34.9	-33.6	-32.3	-29.8	-26.6	-23.3	-20.1	-16.9
270	-44.5	-42.5	-40.6	-38.6	-34.7	-29.7	-24.8	-19.9	-15.0
280	-49.6	-47.2	-44.8	-42.3	-37.5	-31.5	-25.5	-19.4	-13.4
290	-50.8	-48.2	-45.6	-43.1	-37.9	-31.5	-25.1	-18.6	-12.6
300	-48.6	-46.1	-43.8	-41.3	-36.5	-30.5	-24.5	-18.4	-12.4
315	-38.6	-36.9	-35.3	-33.6	-30.3	-26.2	-22.1	-18.0	-13.8
330	-24.0	-23.5	-23.1	-22.6	-21.8	-20.5	-19.3	-18.2	-17.0
340	-13.6	-14.1	-14.5	-15.0	-15.8	-17.0	-18.1	-19.1	-20.4
350	-3.9	-5.2	-6.5	-7.8	-10.3	-13.5	-16.8	-20.0	-23.2
360	3.7	1.7	-0.2	-2.2	-6.1	-11.1	-16.0	-20.9	-25.8

Table XII. (Magnitude of  $\frac{\partial \theta_{r=\sigma}}{\rho g a}$  when  $\varphi=30^\circ$  and  $\frac{\xi}{a}=10$ .)

$\theta \backslash \eta/a$	0	2	4	6	10	13	15
0°	-4.2	-5.9	-7.7	-9.4	-12.8	-15.4	-17.1
10	-2.1	-4.8	-7.4	-10.1	-15.3	-19.3	-22.0
20	-0.8	-4.1	-7.3	-10.6	-17.0	-21.9	-25.2
30	-0.6	-4.1	-7.5	-10.9	-17.8	-23.0	-26.5
45	-2.1	-5.1	-8.1	-11.1	-17.1	-21.5	-24.5
60	-5.3	-7.0	-8.7	-10.5	-13.9	-16.5	-18.2
70	-8.1	-8.7	-9.3	-9.9	-11.1	-12.0	-12.6
80	-11.2	-10.6	-10.0	-9.4	-8.2	-7.3	-6.7
90	-14.1	-12.4	-10.6	-8.9	-5.5	-2.9	-1.2
100	-16.9	-14.2	-11.6	-8.9	-3.7	0.3	3.0
110	-18.7	-15.4	-12.2	-8.9	-2.5	2.4	5.7
120	-19.7	-16.2	-12.8	-9.4	-2.5	2.7	6.2
135	-19.2	-16.2	-13.2	-10.2	-4.2	0.2	3.2
150	-16.2	-14.5	-12.8	-11.0	-7.6	-5.0	-3.3
160	-13.0	-12.4	-11.8	-11.2	-10.0	-9.1	-8.5
170	-9.3	-9.9	-10.5	-11.1	-12.3	-13.2	-13.8
180	-5.8	-7.5	-9.3	-11.0	-14.4	-17.0	-18.7
190	-2.5	-5.2	-7.8	-10.5	-15.7	-19.7	-22.4
200	0.1	-3.2	-6.4	-9.7	-16.1	-21.0	-24.3
210	0.6	-2.9	-6.3	-9.7	-16.6	-21.8	-25.3
225	-0.7	-3.7	-6.7	-9.7	-15.7	-20.1	-23.1
240	-4.7	-6.4	-8.1	-9.9	-13.3	-15.9	-17.6
250	-8.5	-9.1	-9.7	-10.3	-11.5	-12.4	-13.0
260	-12.4	-11.8	-11.2	-10.6	-9.4	-8.5	-7.9
270	-15.9	-14.2	-12.4	-10.7	-7.3	-4.7	-3.0
280	-18.5	-15.8	-13.2	-10.5	-5.3	-1.3	1.4
290	-20.1	-16.8	-13.6	-10.3	-3.9	1.0	4.3
300	-20.3	-16.8	-13.4	-10.0	-3.1	2.1	5.6
315	-18.0	-15.0	-12.0	-9.0	-3.0	1.4	4.4
330	-13.8	-12.1	-10.4	-8.6	-5.2	-2.6	-0.9
340	-10.4	-9.8	-9.2	-8.6	-7.4	-6.5	-5.9
350	-7.1	-7.7	-8.3	-8.9	-10.1	-11.0	-11.6
360	-4.2	-5.9	-7.7	-9.4	-12.8	-15.4	-17.1

Table XIII. (Magnitude of  $\frac{\widehat{\theta\theta}_{r=a}}{\rho g a}$  when  $\varphi=30^\circ$  and  $\frac{\xi}{a}=15$ .)

$\theta \backslash \eta/a$	0	2	4	6	10	13	15	20
0°	-6.6	-8.3	-10.1	-11.8	-15.2	-17.8	-19.5	-23.8
10	-3.3	-6.0	-8.8	-11.3	-16.5	-20.5	-23.2	-29.7
20	-1.1	-4.4	-7.6	-10.9	-17.3	-22.2	-25.5	-33.5
30	-0.6	-4.1	-7.5	-10.9	-17.8	-23.0	-26.5	-35.0
45	-2.7	-5.7	-8.7	-11.7	-17.7	-22.1	-25.1	-32.7
60	-7.9	-9.6	-11.3	-13.1	-16.5	-19.1	-20.8	-25.1
70	-12.3	-12.9	-13.5	-14.1	-15.3	-16.2	-16.8	-18.3
80	-17.0	-16.4	-15.8	-15.2	-14.0	-13.1	-12.5	-11.0
90	-21.7	-20.0	-18.2	-16.5	-13.1	-10.5	-8.8	-4.5
100	-25.6	-22.9	-20.3	-17.6	-12.4	-8.4	-5.7	0.8
110	-28.5	-25.2	-22.0	-18.7	-12.3	-7.4	-4.1	3.9
120	-29.7	-26.2	-22.8	-19.4	-12.5	-7.3	-3.8	4.7
135	-28.6	-25.6	-22.6	-19.6	-13.6	-9.2	-6.2	1.4
150	-23.6	-21.9	-20.2	-18.4	-15.0	-12.4	-10.7	-6.0
160	-18.8	-18.2	-17.6	-17.0	-15.8	-14.9	-14.3	-12.8
170	-13.4	-14.0	-14.6	-15.2	-16.4	-17.3	-17.9	-19.4
180	-8.2	-9.9	-11.7	-13.4	-16.8	-19.4	-21.1	-25.4
190	-3.7	-6.4	-9.0	-11.7	-16.9	-20.9	-23.6	-30.1
200	-0.7	-4.0	-7.2	-10.5	-16.9	-21.8	-25.1	-33.1
210	0.6	-2.9	-6.3	-9.7	-16.6	-21.8	-25.3	-33.8
225	-1.3	-4.3	-7.3	-10.3	-16.3	-20.7	-23.7	-31.3
240	-7.3	-9.0	-10.7	-12.5	-15.9	-18.5	-20.2	-24.5
250	-12.7	-13.3	-13.9	-14.5	-15.7	-16.6	-17.2	-18.7
260	-18.2	-17.6	-17.0	-16.4	-15.2	-14.3	-13.7	-12.2
270	-23.5	-21.8	-20.0	-18.3	-14.9	-12.3	-10.6	-6.3
280	-27.4	-24.7	-22.1	-19.4	-14.2	-10.2	-7.5	-1.0
290	-29.9	-26.6	-23.4	-20.1	-13.7	-8.8	-5.5	2.5
300	-30.3	-26.8	-23.4	-20.0	-13.1	-7.9	-4.4	4.1
315	-27.4	-24.4	-21.4	-18.4	-12.4	-8.0	-5.0	2.6
330	-21.2	-19.5	-17.8	-16.0	-12.6	-10.0	-8.3	-4.0
340	-16.2	-15.6	-15.0	-14.4	-13.2	-12.3	-11.7	-10.2
350	-11.2	-11.8	-12.4	-13.0	-14.2	-15.1	-15.7	-17.2
360	-6.6	-8.3	-10.1	-11.8	-15.2	-17.8	-19.5	-23.8

Table XIV. (Magnitude of  $\frac{\theta\hat{\theta}_{r=a}}{\rho ga}$  when  $\varphi=30^\circ$  and  $\frac{\xi}{a}=20$ .)

$\eta/a$ $\theta$	0	2	4	6	10	13	15	20	25
0°	-9.1	-10.8	-12.6	-14.3	-17.7	-20.3	-23.0	-26.3	-30.7
10	-4.4	-7.1	-9.7	-12.4	-17.6	-21.6	-24.3	-30.8	-37.5
20	-1.4	-4.7	-7.9	-11.2	-17.6	-22.5	-25.8	-33.8	-42.0
30	-0.6	-4.1	-7.5	-10.9	-17.8	-23.0	-26.5	-35.0	-43.7
45	-3.4	-6.4	-9.4	-12.4	-18.0	-22.8	-25.8	-33.4	-40.8
60	-10.4	-12.1	-13.8	-15.6	-19.0	-21.6	-23.3	-27.6	-31.9
70	-16.4	-17.0	-17.6	-18.2	-19.4	-20.3			-23.9
80	-23.0	-22.4	-21.8	-21.2	-20.0	-19.1	-18.5	-17.0	-15.5
90	-29.1	-27.5	-25.7	-24.0	-20.6	-18.0	-16.2	-11.9	-7.5
100	-34.5	-31.8	-29.2	-26.5	-21.3	-17.3	-14.6	-8.1	-1.4
110	-38.1	-34.8	-31.6	-28.2	-21.9	-17.0	-13.7	-5.7	2.5
120	-39.7	-36.2	-32.8	-29.4	-22.5	-17.3	-13.8	-5.3	3.4
135	-38.0	-34.9	-31.9	-28.9	-22.9	-18.5	-15.6	-8.0	-0.6
150	-30.7	-29.0	-27.3	-25.5	-22.1	-19.5		-13.1	-9.2
160	-24.7	-24.1	-23.5	-22.9	-21.7	-20.8	-20.2	-18.7	-17.2
170	-17.5	-18.1	-18.7	-19.3	-20.5	-21.4	-22.0	-23.5	-25.0
180	-10.7	-12.4	-14.2	-15.9	-19.3	-21.9	-23.6	-27.9	-32.3
190	-4.8	-7.5	-10.1	-12.8	-18.0	-22.0	-24.7	-31.2	-37.9
200	-1.0	-4.3	-7.5	-10.8	-17.2	-22.1	-25.4	-33.4	-41.6
210	0.6	-2.9	-6.3	-9.7	-16.6	-21.8	-25.3	-33.8	-42.5
225	-2.0	-5.0	-8.0	-11.0	-17.0	-21.4	-24.4	-32.0	-39.4
240	-9.8	-11.5	-13.2	-15.0	-18.4	-21.0	-22.7	-27.0	-31.3
250	-16.8	-17.4	-18.0	-18.6	-19.8	-20.7	-21.3	-22.8	-24.3
260	-24.2	-23.6	-23.0	-22.4	-21.2	-20.3	-19.7	-18.2	-16.7
270	-30.9	-29.2	-27.4	-25.7	-22.3	-19.7	-18.0	-13.7	-9.3
280	-36.2	-33.6	-31.0	-28.3	-23.1	-19.1	-16.3	-9.8	-3.1
290	-39.5	-36.2	-33.0	-29.7	-23.3	-18.4	-15.1	-7.1	1.1
300	-40.3	-36.8	-33.4	-30.0	-23.1	-17.9	-14.4	-5.9	2.8
315	-36.7	-33.7	-30.7	-27.7	-21.7	-17.3	-14.3	-6.7	0.7
330	-28.3	-26.6	-24.9	-23.1		-17.1	-15.4	-11.1	-6.8
340	-22.1	-21.5	-20.9	-20.3	-19.1	-18.2	-17.6	-16.1	-14.6
350	-15.3	-15.9	-16.5	-17.1	-18.3	-19.2	-19.8	-21.3	-22.8
360	-9.1	-10.8	-12.6	-14.3	-17.7	-20.3	-22.0	-26.3	-30.7



Table XV. (Magnitude of  $\frac{\widehat{\theta\theta}_{r=a}}{\rho ga}$  when  $\varphi=45^\circ$  and  $\frac{r}{a}=10.$ )

$\theta$ \diagdown $\eta/a$	0	2	4	6	7.5
0°	-8.7	-8.7	-8.7	-8.7	-8.7
10	-8.8	-10.2	-11.5	-12.9	-13.9
20	-9.2	-11.8	-14.3	-16.9	-18.9
30	-9.7	-13.2	-16.6	-20.1	-22.7
45	-10.5	-14.5	-18.5	-22.5	-25.5
60	-10.8	-14.3	-17.7	-21.2	-23.8
70	-10.8	-13.4	-15.9	-18.5	-20.5
80	-10.4	-11.8	-13.1	-14.5	-15.5
90	-10.0	-10.0	-10.0	-10.0	-10.0
100	-9.6	-8.2	-6.9	-5.5	-4.5
110	-9.2	-6.6	-4.1	-1.5	0.5
120	-9.2	-5.7	-2.3	1.2	3.8
135	-9.5	-5.5	-1.5	2.5	5.5
150	-10.3	-6.8	-3.4	0.1	2.7
160	-10.8	-8.2	-5.7	-3.1	-1.1
170	-11.2	-9.8	-8.5	-7.1	-6.1
180	-11.3	-11.3	-11.3	-11.3	-11.3
190	-11.2	-12.6	-13.9	-15.3	-16.3
200	-10.8	-13.4	-15.9	-18.5	-20.5
210	-10.3	-13.8	-17.2	-20.7	-23.3
225	-9.5	-13.5	-17.5	-21.5	-24.5
240	-9.2	-12.7	-16.1	-19.6	-22.2
250	-9.2	-11.8	-14.3	-16.9	-18.9
260	-9.6	-11.0	-12.3	-13.7	-14.7
270	-10.0	-10.0	-10.0	-10.0	-10.0
280	-10.4	-9.0	-7.7	-6.3	-5.3
290	-10.8	-8.2	-5.7	-3.1	-1.1
300	-10.8	-7.3	-3.9	-0.4	2.2
315	-10.5	-6.5	-2.5	1.5	4.5
330	-9.7	-6.2	-2.8	0.7	3.3
340	-9.2	-6.6	-4.1	-1.5	0.5
350	-8.8	-7.4	-6.1	-4.7	-3.7
360	-8.7	-8.7	-8.7	-8.7	-8.7

Table XVI. (Magnitude of  $\frac{\widehat{\theta\theta}_{r=a}}{\rho ga}$  when  $\varphi=45^\circ$  and  $\frac{\xi}{a}=15$ .)

$\theta \backslash \eta/a$	0	2	4	6	7.5	10
0°	-13.7	-13.7	-13.7	-13.7	-13.7	-13.7
10	-13.8	-15.2	-16.5	-17.9	-18.9	-20.6
20	-14.2	-16.8	-19.3	-21.9	-23.9	-27.1
30	-14.7	-18.2	-21.6	-25.1	-27.7	-32.0
45	-15.5	-19.5	-23.5	-27.5	-30.5	-35.5
60	-15.8	-19.3	-22.7	-26.2	-28.8	-33.1
70	-15.8	-18.4	-20.9	-23.5	-25.5	-28.7
80	-15.4	-16.8	-18.1	-19.5	-20.5	-22.2
90	-15.0	-15.0	-15.0	-15.0	-15.0	-15.0
100	-14.6	-13.2	-11.9	-10.5	-9.5	-7.8
110	-14.2	-11.6	-9.1	-6.5	-4.5	-1.3
120	-14.2	-10.7	-7.3	-3.8	-1.2	3.1
135	-14.5	-10.5	-6.5	-2.5	0.5	7.5
150	-15.3	-11.8	-8.4	-4.9	-2.3	2.0
160	-15.8	-13.2	-10.7	-8.1	-6.1	-2.9
170	-16.2	-14.8	-13.5	-12.1	-11.1	-9.4
180	-16.3	-16.3	-16.3	-16.3	-16.3	-16.3
190	-16.2	-17.6	-18.9	-20.3	-21.3	-23.0
200	-15.8	-18.4	-20.9	-23.5	-25.5	-28.7
210	-15.3	-18.8	-22.2	-25.7	-28.3	-32.6
225	-14.5	-18.5	-22.5	-26.5	-29.5	-34.5
240	-14.2	-17.7	-21.1	-24.6	-27.2	-31.5
250	-14.2	-16.8	-19.3	-21.9	-23.9	-27.1
260	-14.6	-16.0	-17.3	-18.7	-19.7	-21.4
270	-15.0	-15.0	-15.0	-15.0	-15.0	-15.0
280	-15.4	-14.0	-12.7	-11.3	-10.3	-8.6
290	-15.8	-13.2	-10.7	-8.1	-6.1	-2.9
300	-15.8	-12.3	-8.9	-5.4	-2.8	1.5
315	-15.5	-11.5	-7.5	-3.5	-0.5	4.5
330	-14.7	-11.2	-7.8	-4.3	-1.7	2.6
340	-14.2	-11.6	-9.1	-6.5	-4.5	-1.3
350	-13.8	-12.4	-11.1	-9.7	-8.7	-7.0
360	-13.7	-13.7	-13.7	-13.7	-13.7	-13.7



Table XVIII (Magnitude of  $\frac{\widehat{\theta}\theta_{r=a}}{\rho ga}$  when  $\varphi=60^\circ$  and  $\frac{\xi}{a}=10$ .)

$\theta \backslash \eta/a$	0	2	3.5	$\theta \backslash \eta/a$	0	2	3.5
0°	-4.2	-2.4	-1.0	190	-9.4	-8.8	-8.3
10	-7.0	-6.4	-5.9	200	-13.0	-13.6	-14.1
20	-10.4	-11.0	-11.5	210	-16.2	-18.0	-19.3
30	-13.8	-15.6	-16.9	225	-19.1	-22.1	-24.3
45	-18.1	-21.1	-23.3	240	-19.7	-23.1	-25.7
60	-20.3	-23.5	-26.0	250	-18.7	-21.9	-24.5
70	-20.1	-23.3	-25.9	260	-16.8	-19.4	-21.4
80	-18.6	-21.2	-23.2	270	-14.1	-15.9	-17.3
90	-15.9	-17.7	-19.1	280	-11.2	-11.8	-12.3
100	-12.4	-13.0	-13.5	290	-8.2	-7.6	-7.1
110	-8.4	-7.8	-7.3	300	-5.3	-3.5	-2.2
120	-4.7	-2.9	-1.6	315	-2.1	0.9	3.1
135	-0.7	2.3	4.5	330	-0.6	2.8	5.4
150	0.6	4.0	6.6	340	-0.8	2.5	5.0
160	-0.4	2.8	5.4	350	-2.0	0	2.6
170	-2.6	0	2.0	360	-4.2	-2.4	-1.0
180	-5.8	-4.0	2.6				

Table XIX. (Magnitude of  $\frac{\widehat{\theta}\theta_{r=a}}{\rho ga}$  when  $\varphi=60^\circ$  and  $\frac{\xi}{a}=10$ .)

$\theta \backslash \eta/a$	0	2	3.5	6	$\theta \backslash \eta/a$	0	2	3.5	6
0°	-6.7	-4.9	-3.5	-1.5	190	-13.5	-12.9	-12.4	-11.7
10	-11.1	-10.5	-10.0	-9.3	200	-18.8	-19.4	-19.9	-20.6
20	-16.2	-16.8	-17.3	-18.0	210	-23.6	-25.4	-26.7	-28.8
30	-21.2	-23.0	-24.3	-26.4	225	-28.5	-31.5	-33.7	-37.2
45	-27.5	-30.5	-32.7	-36.2	240	-29.7	-33.1	-35.7	-40.0
60	-30.3	-33.7	-36.3	-40.6	250	-28.5	-31.7	-34.3	-38.3
70	-29.9	-33.1	-35.7	-39.7	260	-25.6	-28.2	-30.2	-33.5
80	-27.4	-30.0	-32.0	-35.3	270	-21.5	-23.3	-24.7	-26.7
90	-23.5	-25.3	-26.7	-28.7	280	-17.1	-17.7	-18.2	-18.9
100	-18.3	-18.9	-19.4	-20.1	290	-12.4	-11.8	-11.3	-10.6
110	-12.6	-12.0	-11.5	-10.8	300	-7.9	-6.1	-4.8	-2.7
120	-7.3	-5.5	-4.2	-2.1	315	-3.1	-0.1	2.1	5.6
135	-1.7	1.3	3.5	7.0	330	-0.6	2.8	5.4	9.7
150	0.6	4.0	6.6	10.9	340	-1.1	2.1	4.7	8.7
160	-0.7	2.5	5.1	9.1	350	-3.2	-0.6	1.4	4.7
170	-3.8	-1.2	0.8	4.1	360	-6.7	-4.9	-3.5	-1.5
180	-8.3	-6.5	-5.1	-3.1					

Table XX. (Magnitude of  $\frac{\widehat{\theta\theta}_{r=a}}{\rho g a}$  when  $\varphi=60^\circ$  and  $\frac{\xi}{a}=20$ .)

$\theta \backslash \eta/a$	0	2	3.5	6	8
0°	-9.1	-7.3	-5.9	-3.9	-2.2
10	-15.2	-14.6	-14.1	-13.4	-12.8
20	-22.1	-22.7	-23.2	-23.9	-24.5
30	-28.7	-30.5	-31.8	-33.9	-35.6
45	-36.8	-39.8	-42.0	-45.5	-48.8
60	-40.3	-43.7	-46.3	-50.6	-54.1
70	-39.5	-42.7	-45.3	-49.3	-52.5
80	-36.2	-38.8	-40.8	-44.1	-46.8
90	-31.0	-32.8	-34.2	-36.2	-37.9
100	-24.2	-24.8	-25.3	-26.0	-26.6
110	-16.7	-16.1	-15.6	-14.9	-14.3
120	-9.8	-8.0	-6.7	-4.6	-2.9
135	-2.1	0.9	3.1	6.6	9.9
150	0.6	4.0	6.6	10.9	14.4
160	-1.0	2.2	4.8	8.8	12.0
170	-4.3	-1.7	0.3	3.6	6.3
180	-9.1	-7.3	-5.9	-3.9	-2.2
190	-17.6	-17.0	-16.5	-15.8	-15.2
200	-24.7	-25.3	-25.8	-26.5	-27.1
210	-31.1	-32.9	-34.2	-36.3	-38.0
225	-37.8	-40.8	-43.0	-46.5	-49.8
240	-39.7	-43.1	-45.7	-50.0	-53.5
250	-38.1	-41.3	-43.9	-47.9	-51.1
260	-34.4	-37.0	-39.0	-42.3	-45.0
270	-29.2	-31.0	-32.4	-34.4	-36.1
280	-23.0	-23.6	-24.1	-24.8	-25.4
290	-16.5	-15.9	-15.4	-14.7	-14.1
300	-10.4	-8.6	-7.3	-5.2	-3.5
315	-3.5	-0.5	1.7	5.2	8.5
330	-0.6	2.8	5.4	9.7	13.2
340	-1.4	1.8	4.4	8.4	11.6
350	-4.3	-1.7	0.3	3.6	6.3
360	-9.1	-7.3	-5.9	-3.9	-2.2

Table XXI. (Magnitude of  $\frac{\widehat{\theta\theta}_{r=a}}{\rho ga}$  when  $\varphi=70^\circ$  and  $\frac{\xi}{a}=10$ .)

$\theta \backslash \eta/a$	0	2	$\theta \backslash \eta/a$	0	2
0°	2.0	4.0	190	-3.1	-1.9
10	-1.7	-0.5	200	-8.4	-8.0
20	-6.2	-5.8	210	-13.9	-14.4
30	-11.4	-11.8	225	-20.9	-22.5
45	-18.7	-20.3	240	-24.7	-27.1
60	-24.1	-26.5	250	-25.1	-27.7
70	-25.5	-28.1	260	-23.7	-26.1
80	-25.1	-27.5	270	-20.8	-22.8
90	-22.8	-24.8	280	-16.6	-17.8
100	-18.6	-19.8	290	-11.9	-12.3
110	-13.5	-13.9	300	-7.0	-6.6
120	-7.6	-7.2	315	-0.5	1.1
135	0.1	1.7	330	3.7	6.1
150	5.1	7.5	340	4.7	7.3
160	5.6	8.5	350	4.1	6.5
170	4.7	7.1	360	2.0	4.0
180	1.6	3.6			

Table XXII. (Magnitude of  $\frac{\widehat{\theta\theta}_{r=a}}{\rho ga}$  when  $\varphi=70^\circ$  and  $\frac{\xi}{a}=15$ .)

$\theta \backslash \eta/a$	0	2	4	$\theta \backslash \eta/a$	0	2	4
0°	2.8	4.8	6.7	190	-4.2	-3.0	-1.6
10	-2.8	-1.6	-0.2	200	-12.1	-11.7	-11.2
20	-9.9	-9.5	-9.0	210	-20.3	-20.7	-21.2
30	-17.7	-18.1	-18.6	225	-30.9	-32.5	-34.2
45	-28.7	-30.3	-32.0	240	-36.9	-39.5	-41.7
60	-36.3	-38.7	-41.1	250	-37.8	-40.4	-42.9
70	-38.2	-40.8	-43.3	260	-35.8	-38.2	-40.6
80	-37.2	-39.6	-42.0	270	-31.6	-33.6	-35.5
90	-33.6	-35.6	-37.5	280	-25.4	-26.6	-28.0
100	-27.4	-28.2	-30.0	290	-18.2	-18.6	-19.1
110	-19.8	-20.2	-20.7	300	-10.7	-10.3	-9.8
120	-11.3	-10.9	-10.4	315	-2.7	-1.1	0.6
135	0.1	1.7	3.4	330	6.0	8.4	10.8
150	7.3	9.7	12.1	340	7.4	10.0	12.5
160	8.6	11.2	13.7	350	6.2	8.6	11.0
170	6.8	9.2	11.6	360	2.8	4.8	6.7
180	2.4	4.4	6.3				

Table XXIII. (Magnitude of  $\frac{\widehat{\theta}_{r=a}}{\rho g a}$  when  $\varphi=70^\circ$  and  $\frac{\xi}{a}=20.$ )

$\theta \backslash \eta/a$	0	2	4	6
0°	3.7	5.7	7.6	9.6
10	-4.0	-2.8	-1.4	-0.1
20	-13.6	-12.2	-12.7	-12.3
30	-24.0	-24.4	-24.9	-25.3
45	-38.6	-40.2	-41.9	-43.6
60	-48.5	-50.9	-53.3	-55.7
70	-50.9	-53.5	-56.0	-58.6
80	-49.4	-51.8	-54.2	-56.6
90	-44.5	-46.5	-48.4	-50.4
100	-36.3	-37.5	-38.9	-40.2
110	-26.1	-26.5	-27.0	-27.4
120	-15.0	-14.6	-14.1	-13.7
135	0.0	1.6	3.3	5.0
150	9.5	11.9	14.3	16.7
160	11.3	13.9	16.4	19.0
170	10.0	12.4	14.8	17.2
180	3.3	5.3	7.2	9.2
190	-5.4	-4.2	-2.8	-1.5
200	-15.8	-15.4	-14.9	-14.5
210	-26.6	-27.0	-27.5	-27.9
225	-40.8	-42.4	-44.1	-45.8
240	-49.1	-51.5	-53.9	-56.3
250	-50.5	-53.1	-55.6	-58.2
260	-48.0	-50.4	-52.8	-55.2
270	-42.5	-44.5	-46.4	-43.4
280	-34.3	-35.5	-36.9	-38.2
290	-24.5	-24.9	-25.4	-25.8
300	-14.4	-14.0	-13.5	-13.1
315	-0.6	1.0	2.7	4.6
330	8.1	10.5	12.9	15.3
340	10.1	12.7	15.2	17.8
350	8.4	10.8	13.2	15.6
360	3.7	5.7	7.6	9.6

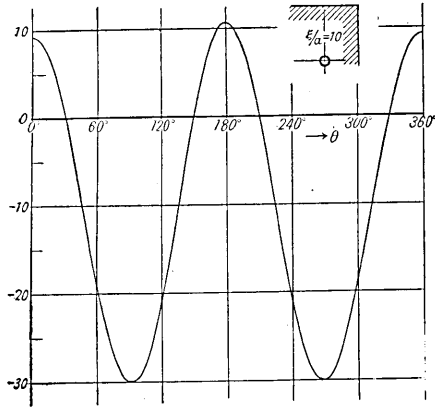


Fig. 22. Magnitude of  $\frac{\widehat{\theta\theta}_{r=a}}{\rho g a}$  when  $\varphi=0^\circ$  and  $\frac{\xi}{a}=10$ .

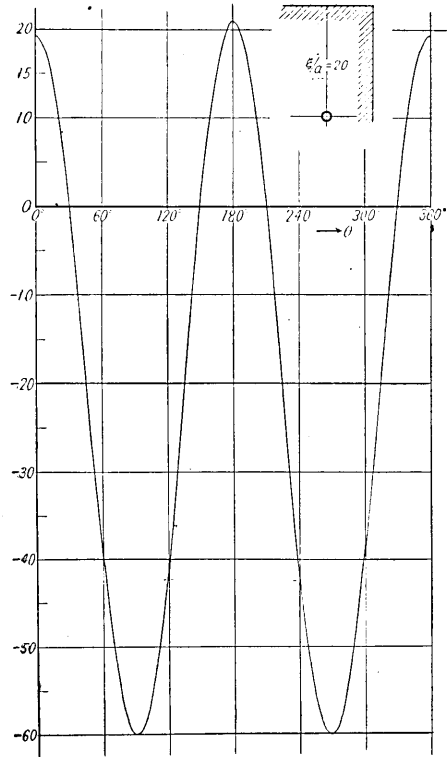


Fig. 24. Magnitude of  $\frac{\widehat{\theta\theta}_{r=a}}{\rho g a}$  when  $\varphi=0^\circ$  and  $\frac{\xi}{a}=20$ .

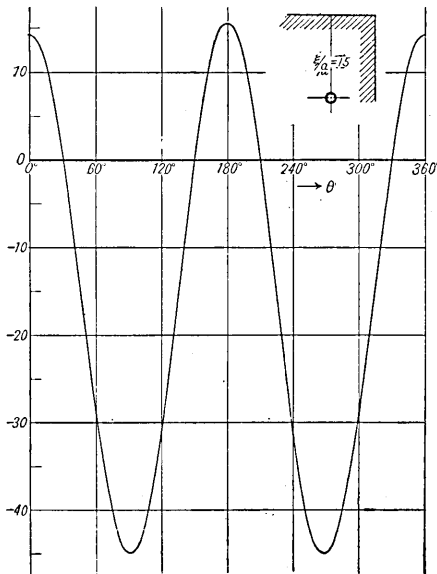


Fig. 23. Magnitude of  $\frac{\widehat{\theta\theta}_{r=a}}{\rho g a}$  when  $\varphi=0^\circ$  and  $\frac{\xi}{a}=15$ .

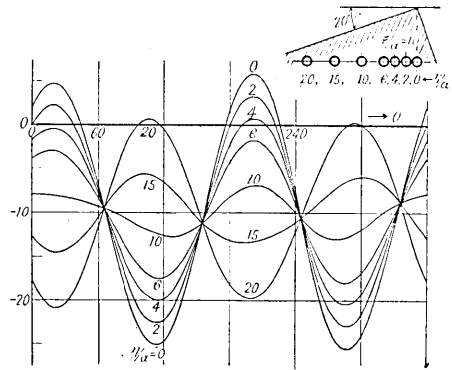


Fig. 25. Magnitude of  $\frac{\widehat{\theta\theta}_{r=a}}{\rho g a}$  when  $\varphi=20^\circ$ , and  $\frac{\xi}{a}=10$ .  
 $(\frac{\eta}{a}=0, 2, 4, 6, 10, 15, 20.)$



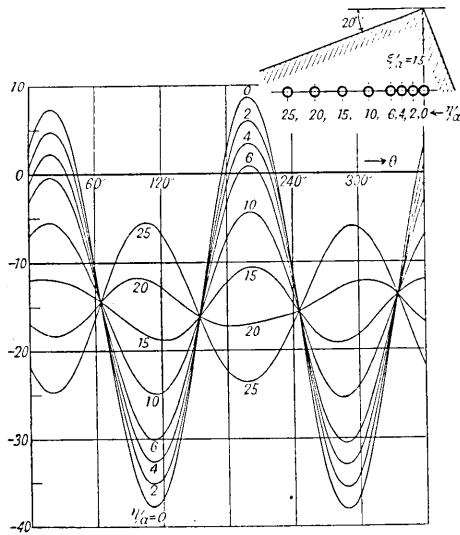


Fig. 26. Magnitude of  $\widehat{\theta\theta}_{r=a}$  when  $\varphi = 20^\circ$  and  $\frac{\xi}{a} = 15^\circ$   
 $(\frac{\eta}{a} = 0, 2, 4, 6, 10, 15, 20, 25.)$

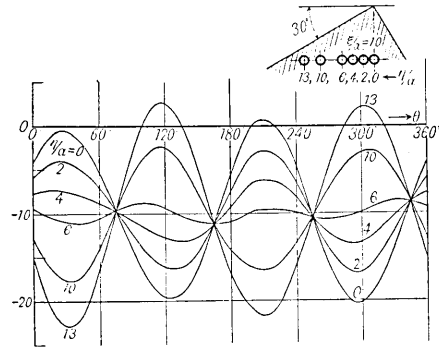


Fig. 28. Magnitude of  $\widehat{\theta\theta}_{r=a}$  when  $\varphi = 30^\circ$  and  $\frac{\xi}{a} = 10^\circ$   
 $(\frac{\eta}{a} = 0, 2, 4, 6, 10, 13.)$

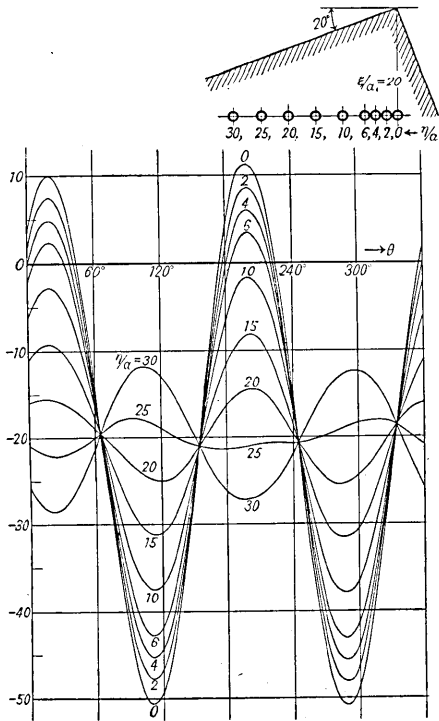


Fig. 27. Magnitude of  $\widehat{\theta\theta}_{r=a}$  when  $\varphi = 20^\circ$  and  $\frac{\xi}{a} = 20^\circ$   
 $(\frac{\eta}{a} = 0, 2, 4, 6, 10, 15, 20, 25, 30.)$

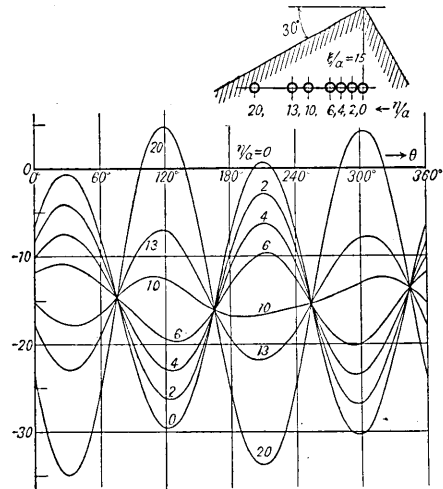


Fig. 29. Magnitude of  $\widehat{\theta\theta}_{r=a}$  when  $\varphi = 30^\circ$  and  $\frac{\xi}{a} = 15^\circ$   
 $(\frac{\eta}{a} = 0, 2, 4, 6, 10, 13, 20.)$

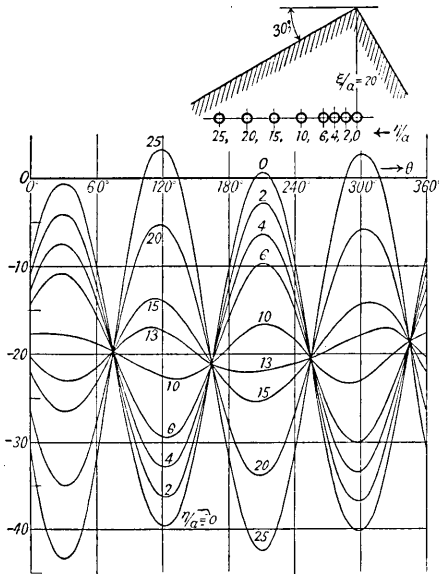


Fig. 30. Magnitude of  $\frac{\partial \theta_{r=a}}{\partial \rho g a}$  when  $\varphi = 30^\circ$  and  $\frac{\xi}{a} = 20$ .  
 ( $\frac{\eta}{a} = 0, 2, 4, 6, 10, 13, 15, 20, 25$ .)

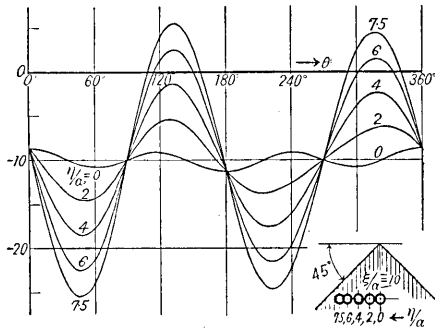


Fig. 31. Magnitude of  $\frac{\partial \theta_{r=a}}{\partial \rho g a}$  when  $\varphi = 45^\circ$  and  $\frac{\xi}{a} = 10$ .  
 ( $\frac{\eta}{a} = 0, 2, 4, 6, 7.5$ .)

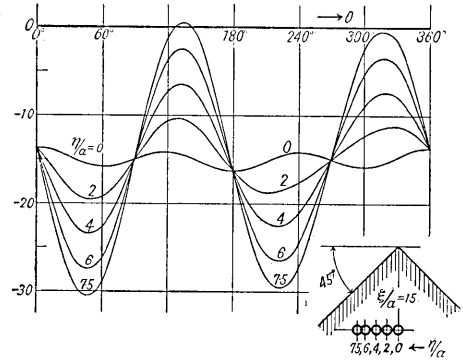


Fig. 32. Magnitude of  $\frac{\partial \theta_{r=a}}{\partial \rho g a}$  when  $\varphi = 45^\circ$  and  $\frac{\xi}{a} = 15$ .  
 ( $\frac{\eta}{a} = 0, 2, 4, 6, 7.5$ .)

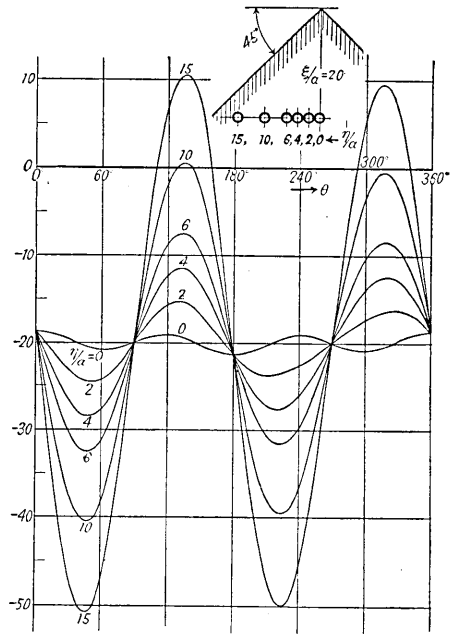


Fig. 33. Magnitude of  $\frac{\partial \theta_{r=a}}{\partial \rho g a}$  when  $\varphi = 45^\circ$  and  $\frac{\xi}{a} = 20$ .  
 ( $\frac{\eta}{a} = 0, 2, 4, 6, 10, 15$ .)

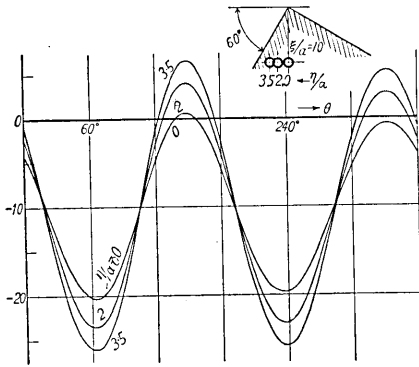


Fig. 34. Magnitude of  $\frac{\widehat{\theta\theta}_{r=a}}{\rho g a}$  when  $\varphi = 60^\circ$  and  $\frac{\xi}{a} = 10$ .  
 $(\frac{\eta}{\alpha} = 0, 2, 3.5.)$

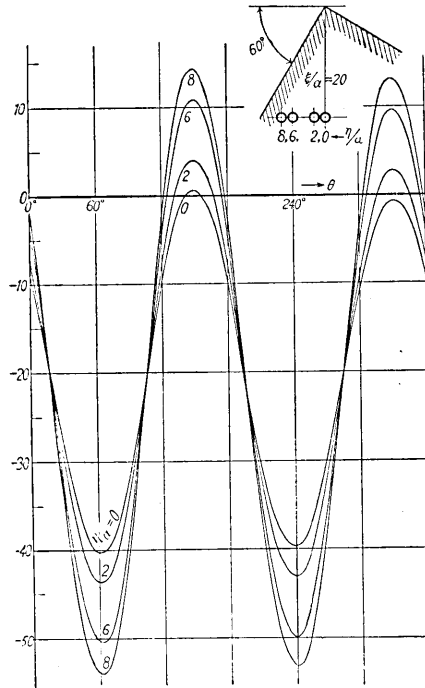


Fig. 36. Magnitude of  $\frac{\widehat{\theta\theta}_{r=a}}{\rho g a}$  when  $\varphi = 60^\circ$  and  $\frac{\xi}{a} = 20$ .  
 $(\frac{\eta}{\alpha} = 0, 2, 6, 8.)$

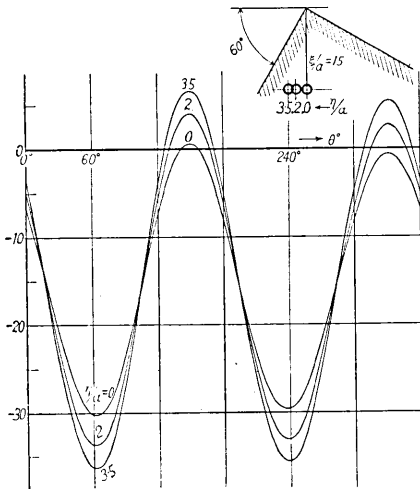


Fig. 35. Magnitude of  $\frac{\widehat{\theta\theta}_{r=a}}{\rho g a}$  when  $\varphi = 60^\circ$  and  $\frac{\xi}{a} = 15$ .  
 $(\frac{\eta}{\alpha} = 0, 2, 3.5.)$

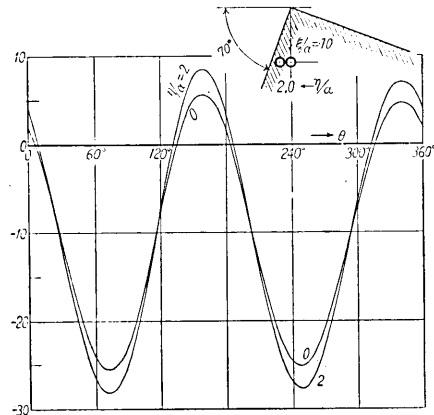


Fig. 37. Magnitude of  $\frac{\widehat{\theta\theta}_{r=a}}{\rho g a}$  when  $\varphi = 70^\circ$  and  $\frac{\xi}{a} = 10$ .  
 $(\frac{\eta}{\alpha} = 0, 2.)$

## 48. 重力の働ける楔形弾性體を貫通する水平圓形孔附近の應力

地震研究所 { 西村源六郎  
高 山 威 雄

重力の作用せる半無限弾性體内にある水平圓形孔及び傾孔附近の應力は山口昇教授、杉原武徳助教授によつて夫々詳しく研究されてゐる。表面の形によつてこれ等圓形孔附近の應力は非常に影響されるものである事は誰も容易に考へ得る事であるが、本論文では、この事に關係して重力が作用してゐる一つの楔形弾性體内に水平圓形孔がある場合、この附近の應力がどのような性質をあらはすものであるかを研究してみた。研究方法は楔形弾性體の表面と圓形孔の面に於ける彈性的條件を完全に満足さす事は非常に煩しい事であるから、圓形孔の面では完全に弾性條件を満足し孔よりへだたるに従つて孔の存在の影響がなくなつてしまふ様な具合にした。楔形弾性體の頂角は直角をなしており、そしてその一つの面が水平面と色々の角をなす場合、圓形孔の弾性體の頂點に對する位置が種々變つた時に、圓形孔の圍りで應力分布がどのような變化を示めすかを論じてある。數計算の結果は可なり面白いと思はれる應力分布の性質を示してゐるが、多少でも參考になる所があれば幸甚である。